ORIGINAL PAPER

Antenatal Exposure to Plastic Pollutants: Study of the Bisphenols and Perfluoroalkyls Effects on Human Stem Cell Models

Giulia Gaggi[1,2] · Andrea Di Credico[1,2] · Federica Barbagallo[3,4] · Patrizia Ballerini[1,5] · Barbara Ghinassi[1,2] ·
Angela Di Baldassarre[1,2]

Abstract

Endocrine disruptors (EDs), such as Bisphenols (BPs) and Perfluoroalkyls (PFs), are a class of plastic pollutants widely used in industrial applications. Human exposure to these molecules usually occurs through ingestion of contaminated food and water. Once entered the human body they can interfere with endogenous hormone signaling, leading to a wide spectrum of diseases. It has been reported that BPs and PFs can cross the placental barrier accumulating in the fetal serum, but the detrimental consequences for human development remain to be clarified. Here we analyze the effects of different doses of bisphenol A and S (BPA, BPS) perfluorooctane sulfonate (PFOS) and perfluorooctanoic acid (PFOA) on proliferation and mitochondrial health on different types of stem cells: through an integrated approach that combines data from pluripotent stem cells (hiPSCs) with that from the "environment" in which the embryo develops (fetal annexes-derived perinatal stem cells) we verified the potential developmental toxicity of the in utero EDs exposure. Data obtained showed that overall, BPs, and PFs tended to increase the proliferation rate of perinatal stem cells; a similar response was observed in hiPSCs exposed to very low doses of BPs and PFs, while at higher concentrations these chemicals were toxic; in addition, both the BPs and the PFs exerted a mitotoxic effects hiPSCs at all the concentration studied. All these data suggest that antenatal exposure to BPs and PFs, also at very low concentrations, may modify the biological characteristics of stem cells present in both the developing fetus and the fetal annexes, thus perturbing normal human development.

Keywords Endocrine disruptors · BPA · BPS · PFOS · PFOA · Antenatal exposure · Human stem cells · Perinatal stem cells · iPSCs

Introduction

Health concern is rising about the immediate- and long-term consequences of human exposure to plastic pollutants that contaminate the environment leaching molecules such as Bisphenols (BPs), in particular Bisphenol A (BPA) and S (BPS), and perfluoroalkyls (PFs), like perfluorooctane sulfonate (PFOS) and perfluorooctanoic acid (PFOA). All these chemical compounds act as endocrine disruptors (EDs) (Benjamin et al. 2017; Shafei et al. 2018). EDs are molecules that mimic or interfere with hormones, impacting the endocrine system and subsequently impairing the animal and human health (Gore et al. 2015; Li et al. 2020); the endocrine system, indeed, underlies nearly all human biological functions and EDs (Shafei et al. 2018; Behr et al. 2018). Although the molecular mechanism has not been completely clarified, it is generally accepted that BPs act as xenoestrogen, binding and activating the estrogen receptors

✉ Angela Di Baldassarre
a.dibaldassarre@unich.it

1 Reprogramming and Cell Differentiation Lab, Center for Advanced Studies and Technology (CAST), 66100 Chieti, Italy

2 Department of Medicine and Aging Sciences, "G. D'Annunzio" University of Chieti-Pescara, 66100 Chieti, Italy

3 Faculty of Medicine and Surgery, Kore University of Enna, Enna, Italy

4 Department of Experimental Medicine, Sapienza University of Rome, Rome, Italy

5 Department of Innovative Technologies in Medicine and Dentistry, "G. D'Annunzio" University, Chieti, Italy

(ER) α and β that, in turn, bind the estrogen response element (ERE) in the DNA promoter region of ER-target genes, inducing their transcription. ER-target genes are mainly involved in cell proliferation and regulation of WNT and TGFβ signaling pathways (Li et al. 2018). On the other side, when BPs are present at very low doses (pM), they can bind also the non-classical G-coupled estrogen receptor, activating the production of cAMP and the ERK1/2/c-fos cascade that usually induces cell migration and proliferation and it is a marker of poor prognosis in many cancers (Fenichel et al. 2013). Similarly, PFs can bind the ERs in addition to the androgen receptor (AR) and thyroid hormone receptors (TRs): PFOS has been shown to induce estradiol synthesis and reduce testosterone production, altering the expression of many steroidogenic genes and many members of the cytochrome P450 family (Du et al. 2013); PFOA can bind the soluble AR impairing its nuclear translocation and consequently disrupting the expression of androgen-responsive genes (Tachachartvanich et al. 2022); evidence also support the idea that PFs may act as agonists of the TRs altering the neuronal development in the prenatal life and the metabolism regulation in post-natal life (Coperchini et al. 2021).

BPs and PFs are leached by many daily objects; in particular, BPs are widely used in plastic products including food storage containers, while PFs are commonly used in industrial applications, such as non-stick pans, paper, and textile coatings. BPA is a ubiquitous compound that is a pseudo-persistent chemical; despite its short half-life, it is considered one of the most common EDs in the environment, being constantly released into it. After ingestion, BPA is converted into its glucuronide form, which is biologically inactive. Despite that, the parent and biologically active BPA form can still be detected in the body and cause alterations in the reproductive organs of developing mice embryos (Schönfelder et al. 2002). BPA has gradually been replaced by its analogs; in particular, BPS is widely used because it has higher thermal stability and leaches to a lesser degree from plastics; however, being structurally similar to BPA, also BPS raises doubts relative to its safety for human health, particularly during pregnancy and prenatal life (Abrantes-Soares et al. 2022), as it was detected at greater concentrations than BPA in human samples and in both maternal and fetal plasma (Zhao et al. 2018; Pan, et al. 2020). Even the exposures to PFs are geographically global with significant discrepancies among countries and continents (Liu et al. 2020a): PFOS is a ubiquitous compound widely used in industrial products that accumulates in the liver altering lipid metabolism and hormone regulation. PFOS is very stable in the environment and its half-life in humans was estimated at 5.4 years (Lau et al. 2006). It has been also detected in breast milk, maternal serum, and cord blood. Like PFOS, PFOA is a very stable environmental contaminant: it is absorbed, not known to

be metabolized, and poorly eliminated. Prenatal exposure to PFOA is associated with lower birth weight (Peterson et al. 2022). While the levels of PFOS and PFOA have declined since 2000, their levels exceed those of some major environmental toxins in maternal blood (Liu et al. 2020a).

As all humans, also pregnant women are unavoidably and unintentionally exposed BPs or PFs using daily products. Pregnancy is one of the most susceptible periods to pollutants as in utero exposures to xenobiotics may compromise early developmental processes and predispose the fetus to biological modifications that can cause adverse health risks both immediately and also later in life (Napso et al. 2021; Ghassabian et al. 2022). BPs can be transferred via the placenta from the mother to the fetus; studies performed in several European, American, and Asiatic countries evidenced the BPs presence in a variety of biological samples, such as in maternal and cord blood, maternal urine, placenta, and amniotic fluid (Abrantes-Soares et al. 2022). Similarly, PFs have been detected in maternal blood, cord blood, breast milk, placenta, and other fetal samples and their concentrations are relatively high in blood samples (maternal, cord, and infant) and lower in breast milk (Liu et al. 2020a). Although maternal and infant exposure to BPs and PFs represent a global problem, the extent of BPs and PFs health impact remains to be clarified: it is very difficult, indeed, to develop ethical models that mimic human in utero exposure to EDs. Moreover, data on EDs dose response are still controversial because, like hormones, they activate their receptors in a non-linear manner (Hill et al. 2018).

Human-induced pluripotent stem cells (hiPSCs) are adult cells that have been genetically reprogrammed to an embryonic stem cell (ESC)-like state through the forced expression of pluripotency genes (Oct4, Sox2, Klf4, and cMyc) (Gaggi et al. 2021). In this way, these cells acquired the ability to undergo self-renewal indefinitely and the capacity to differentiate into cells from all three germ layers (Baldassarre et al. 2018; Credico et al. 2021), both in vivo and in vitro, becoming morphologically, molecularly and epigenetically almost indistinguishable from ESCs isolated from a blastocyst (Parrotta et al. 2017). The use of hiPSCs is generally preferred to hESCs since their isolation does not arise any ethical issue related to the destruction of a human blastocyst, which is why hESCs, use is forbidden in many countries (Lo and Parham 2009). On the other side, human fetal membrane mesenchymal stromal cells (hFM-MSCs) and human amniotic fluid stem cells (hAFSCs) belong to perinatal stem cells; they are isolated from fetal annexes (amniotic fluid and amniochorionic membrane of the placenta, respectively) during easy medical routine such as amniocentesis or after term delivery; being isolated from discarded material, their use does not raise ethical concerns. They express many pluripotent state-associated markers and show intermediate

biological characteristics between the ESCs and the adult stem cells ((Gaggi et al. 2019, 2022)) (Gaggi et al. 2020a).

The aim of this study is to analyze the consequences of antenatal exposure to BPs and PFs on the fetus's health: for this purpose, the hiPSCs and perinatal stem cells will be treated with different doses of BPs and PFs and the possible effects on their proliferation and mitochondrial health will be analyzed. In our study, the hiPSCs offer a reliable model to investigate the effects of EDs on embryonic-like cells without the controversial use of hESCs. On the other side, since hAFSCs and hFM-MSCs are isolated from the fetal annexes, they allow us to study the impact of EDs on the "environment" where the embryo develops. Indeed, it is well known that a healthy placenta is essential for a successful pregnancy and its alteration is associated with poor outcomes and impaired fetal development (Zhang et al. 2021; Hulme et al. 2018). This integrated approach might be the optimal model to clarify the potential developmental toxicity of the in utero EDs exposure.

Material and Methods

Human Cell Cultures and Treatments

Normal hiPSCs were purchased from iXCells Biotechnologies (San Diego, USA) and cultured on Matrigel (Corning, Sommerville, MA, USA) pre-coated 6-well plates (Corning Sommerville, MA, USA) in mTeSR Plus medium (STEMCELL Technologies, Vancuver, Canada), following the manufacturer's procedures.

Placenta and amniotic fluid samples were obtained after written informed consent in accordance with the Declaration of Helsinki. All samples had normal diploid karyotypes. The study was approved by the ethics committee of the "G. d'Annunzio" University of Chieti-Pescara, ASL Lanciano-Chieti-Vasto, Italy and all experiments were performed in accordance with relevant guidelines and regulations. The hAFSCs were isolated as previously described (Antonucci et al. 2014) from 3 women undergoing amniocentesis for prenatal diagnosis at 16–17 weeks of pregnancy; cells were cultured in Iscove's modified Dulbecco's medium (IMDM) supplemented with 20% fetal bovine serum (FBS), 1% penicillin/streptomycin, 2 mM l-glutamine, and 5 ng/mL bFGF. The hFM-MSCs were isolated from the term placentas of 3 healthy donor mothers as previously described (Gaggi et al. 2022). Cells were cultured in DMEM 10% FBS, 1% penicillin/streptomycin, and 2 mM l-glutamine.

BPA, BPS, PFOS, or PFOA (Wellington Laboratories, Guelph, Canada) dissolved in methanol were serial diluted in culture media. Cells were then exposed to increasing concentration (0.01, 0.1, 1, and 2 μM) of BPA, BPS, PFOS, or PFOA for 24 or 48 h.

Analysis of Impedance

hFM-MSCs, hAFSCs, and hiPSCs were seeded at $15–20 \times 10^5$ on 96-Well CytoView MEA plate (Axion Biosystems, Atlanta, GA, USA). When the cells were in the logarithmic growth phase, sample were treated with the EDs (BPA, BPS, PFOS, or PFOA) ranging from 0.01 μM to 2 μM for 48 h. Impedance values were recorded in real time by Maestro Edge (Axion Biosystems, Atlanta, USA) using the Impedance Module of Axion Integrated Studio software (Axion Biosystems, Atlanta, USA). The resistance was set at 41.5 kHz.

Immunofluorescence Analysis of Ki67 Expression

hFM-MSCs, hAFSCs, and hiPSCs were seeded at $15–20 \times 10^5$ cell/well in μ-Slide 8 Well (Ibidi, Germany). Chamber slides were pre-coated with Matrigel 1:50, when required. During the exponential phase, cells were treated with BPA, BPS, PFOS, and PFOA ranging from 0.01 μM to 2 μM for 24 h. Then immunofluorescence analysis was performed as previously described (Gaggi et al. 2020b). Briefly, cells were fixed in paraformaldehyde 4% and permeabilized by Triton 0.5%. After blocking with BSA 5%, cells were stained with anti-Ki67 antibody 1:100 Alexa fluor 488 conjugated (Thermo Fisher Scientific) overnight at 4 °C. Nuclei were counterstained with DAPI 1:1000 (Thermo Fisher Scientific). Pictures were acquired by EVOS M7000 (Thermo Fisher Scientific) and analyzed by Celleste Image Analysis Software (Thermo Fisher Scientific).

Immunofluorescence Analysis of Mitochondrial Membrane Potential

The mitochondrial functionality was analyzed by HCS Mitochondrial Health Kit (Thermo Fisher Scientific) following the manufacturer's procedures. Briefly, hFM-MSCs, hAFSCs, and hiPSCs were treated with BPA, BPS, PFOS, and PFOA ranging from 0.01 μM to 2 μM for 24 h; cells were then incubated with the MitoStain for 30 min at 37 °C and then fixed in paraformaldehyde 4% for 10 min; nuclei were counterstained by Hoechst 33,342. To quantify the fluorescence, 9 different fields for each sample were acquired by EVOS M7000 (Thermo Fisher Scientific) and analyzed by Celleste Image Analysis Software (Thermo Fisher Scientific) (Giacomo et al. 2005).

Statistical Analysis

All data are presented as the mean ± SD of 3 independent experiments. The statistical analysis was performed by Prism 9 (GraphPad, San Diego, CA, USA) using the Student's T Test. The level of significance was set at $p < 0.05$.

Experimental Design

The potential BPs and PFs developmental toxicity have been evaluated by treating the hiPSCs and the perinatal stem cells with doses of BPA, BPS, PFOS, and PFOA ranging from 0.01 uM to 2 uM and analyzing their effects on cell proliferation and on mitochondria health.

The effects of the EDs on cell growth rate and viability were monitored in real time measuring the cell impedance (ohms, Ω) by means of microelectrodes embedded in the culture surface of each well; cells growth was detected as an increase in impedance, while cell death or detachment determine an impedance decrease; continuous data have been registered up to 48 h to evaluate the cell-drug responses over time. The EDs effects on the proliferative activity were also immunocytochemically evaluated by the expression of the nuclear protein Ki67, a well-recognized marker of proliferation (Sun and Kaufman 2018). Finally, to investigate if different doses of EDs could be detrimental for mitochondria activity and metabolism, we used the MitoHealth fluorescent stain; this dye accumulates in active and healthy mitochondria that then appear brilliantly red; changes in the mitochondrial membrane potential are detected as a staining reduction.

Results

Dose–Response Effects of BPA on Perinatal Stem Cells and hiPSCs

hFM-MSCs were treated with increasing doses (0.01 uM, 0.1 uM, 1 uM, and 2 uM) of BPA up to 48 h and the impedance values were in vivo monitored. We observed an increase in the cell growth in all BPA-treated samples; this effect, that become evident soon after the treatment (6–12 h), was dose dependent, with the more elevated impedance values recorded at the higher BPA concentration (1 and 2 μM) (Fig. 1A and Table 1). The exposure of the cells to 0.1-μM BPA was less affective on cell proliferation than the 0.01 μM (Table 1). The hFM-MSCs proliferative response to BPA was confirmed by morphological evaluation of the Ki67 expression, a typical marker of cell proliferation highly expressed in G2-M phases of the cell cycle (Sobecki et al. 2016); as reported in Fig. 1B, the percentage of the nuclei Ki67^{+} was significantly modified in all 24-h BPA-treated samples. Finally, mitochondria health in control and EDs-treated cells was evaluated with MitoHealth, a specific fluorescent probe that stores inside the active mitochondria; the analysis of the fluorescence intensities evidenced a reduction of the mitochondrial

staining upon a 24-h BPA exposure at all the concentration analyzed, except for the 0.1 μM (Fig. 1C).

To test whether other fetal annexes-derived stem cells displayed a similar sensitivity to BPA, the same set of experiments was performed on the hAFSCs. MEA array evidenced that, although BPA after 24 h enhanced the cell proliferation rate, no differences in the impedance values were recorded after 48 h in all samples, except for BPA 0.1 μM (Fig. 2A and Table 1); the observation that low concentration of BPA initially drives cells toward proliferation was confirmed by the Ki67 expression that increased after 24-h exposure in 0.01- and 0.1-μM BPA-treated samples (Fig. 2B). The potential BPA mitotoxicity was then studied; the fluorescence quantification of the mitochondrial staining evidenced that 24-h exposure to very low (0.01 μM) or intermediate (1 μM) concentrations altered the mitochondrial membrane (Fig. 2C).

The biological effects of scalar dose of BPA were finally tested on hiPSCs. Unlike the perinatal stem cells, the proliferation rate of hiPSCs was not affected by BPA except after 48 h at very low doses (0.01 μM); no changes in the percentage of Ki67^{+} cells were detected (Fig. 3A, 3B and Table 1.) On the other side, this chemical caused a dramatic reduction of mitochondrial membrane potential (Fig. 3C) at all concentration tested.

These results indicated that BPA affected, even if at different extents, the proliferation rate and the mitochondria health of the fetal annexes-derived stem cells (more hFM-MSCs than hAFSCs); on the other hand, hiPSCs responded only to very low doses of BPA by increasing the growth rate, but BPA exerted in these cells an important mitotoxicity.

Dose–Response Effects of BPS on Perinatal Stem Cells and hiPSCs

Like BPA, BPS exposure significantly increased the hFM-MSC proliferation at all the tested concentration; this effect was evident earlier in presence of lower BPS concentrations (Fig. 4A and Table 1). This observation was confirmed by the analysis of the Ki67 expression that was significantly higher in the nuclei of the 0.01 μM-, 0.1 μM-, and 1 μM-treated samples (Fig. 4B). No significant changes in mitochondria health were observed at any tested concentration (Fig. 4C).

The same tests were then performed on hAFSCs that, like hFM-MSCs, increased their proliferation rate in response to the pollutant; this effect, earlier detectable for very low and low doses, was clearly manifest after 48 h for all doses except for 2 μM (Fig. 5A and Table 1). The observation of the early effects evoked by very low and low doses of BPS on the proliferative activity was then supported by the immunofluorescence analysis that showed an increased Ki67 expression after 24-h exposure to 0.01- and 0.1-μM BPS
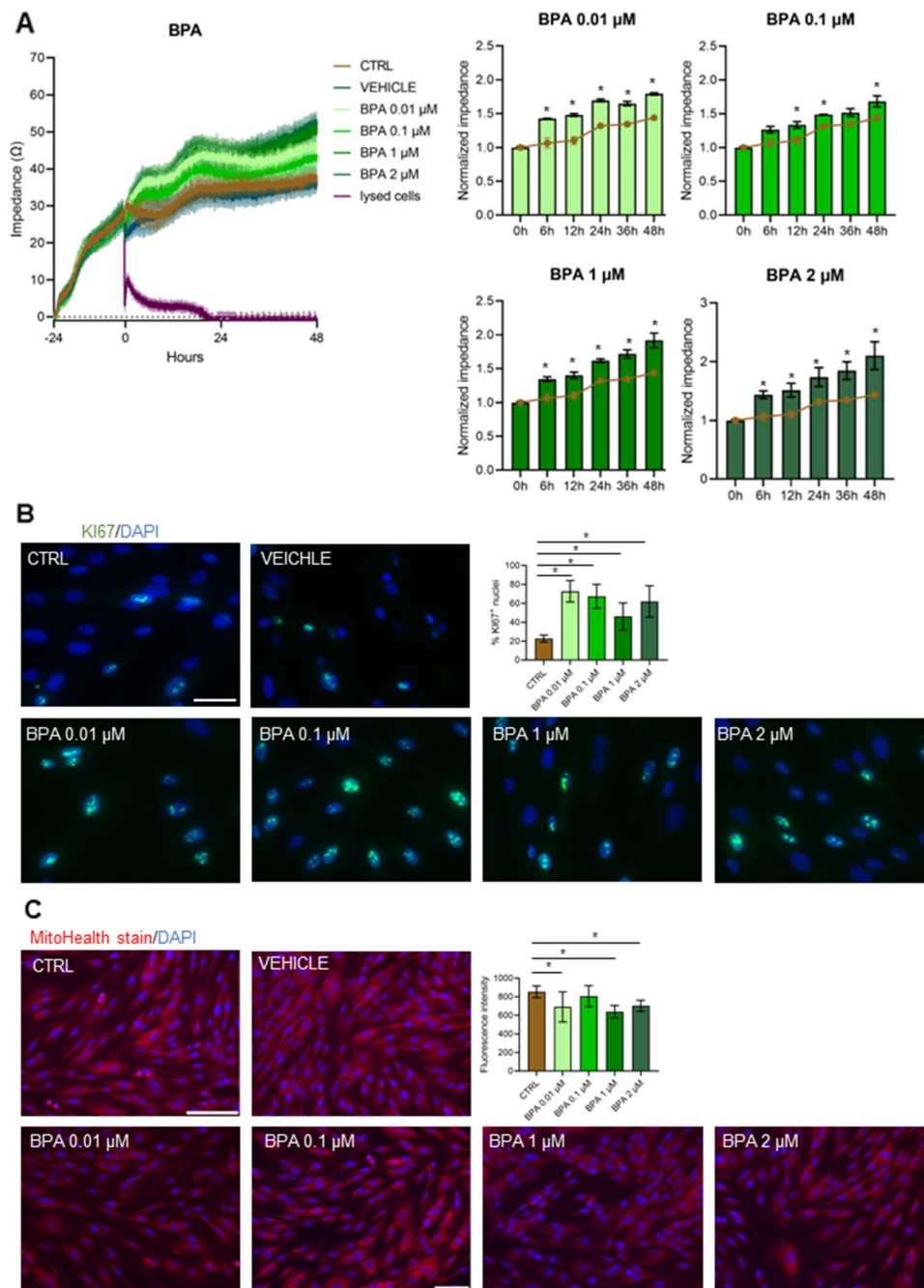
Fig. 1 Dose–response effects of BPA on hFM-MSCs. **A** On day 0 hFM-MSCs were treated with different doses of BPA and the impedance values were monitored in real time up to 48 h. Green lines of increasing intensities, from pale to dark, represent the diverse BPA concentrations, as indicated. Cells not treated (brown line), treated only with the vehicle (dark blue line), or with lysing agents (purple line) represented the experimental controls. *Left panel*: absolute impedance values (expressed in ohms, Ω). Graph is representative of three different experiments. *Right Panel*: Normalized impedance values (Day $0 = 1$) of Control (brown line) or BPA-treated samples (green histograms) at different concentration, as indicated. Data are expressed as mean $\pm$ SD ($n = 3$, $*p < 0.05$ vs Control). **B** Immunocytochemical detection of Ki67 (green fluorescence) in hFM-MSC control cells and after 24-h exposure to vehicle or increasing BPA

concentration. The nuclei were counterstained with DAPI (blue). Original magnification: 40x, scale bar 50 mm. Images are representative of 3 independent experiments. Graph on the right indicates the % of the positive nuclei in the different experimental conditions. Data are expressed as mean $\pm$ SD ($n = 3$, $*p < 0.05$ vs Control). **C** Immunocytochemical detection of mitochondria membrane potential (red fluorescence) in control cells and after 24-h exposure to vehicle only or to different BPA concentration. The nuclei were counterstained with DAPI (blue). Original magnification: 20×, scale bar 100 mm. Images are representative of 3 independent experiments. Graph indicates the fluorescent intensity (absolute values) in the different experimental conditions. Data are expressed as mean $\pm$ SD ($n = 3$, $*p < 0.05$ vs Control)

Table 1 Effects of a 48-h exposure to the diverse pollutants on cell proliferative rate

Pollutant	Doses	Cell type		
		hFM-MSCs	hAFSCs	hiPSCs
BPA	0.01 uM	**1.24**	1.06	**1.15**
	0.1 uM	**1.17**	**1.14**	0.96
	1 uM	**1.33**	0.83	0.93
	2 uM	**1.46**	1.07	1.10
BPS	0.01 uM	**1.12**	**1.15**	**1.14**
	0.1 uM	**1.26**	**1.22**	0.93
	1 uM	**1.26**	**1.21**	*0.70*
	2 uM	**1.20**	1.04	*0.92*
PFOS	0.01 uM	1.12	**1.27**	**1.20**
	0.1 uM	**1.63**	**1.40**	0.98
	1 uM	1.09	**1.17**	1.03
	2 uM	**1.25**	*0.89*	*0.79*
PFOA	0.01 uM	1.10	**1.16**	**1.25**
	0.1 uM	1.10	**1.21**	1.03
	1 uM	1.21	1.26	1.01
	2 uM	**1.14**	1.08	1.00

Data are expressed as fold increase of impedance values relative to control

The bold and italic values represent a significant ($p < 0.05$) increased or decreased fold change vs CTRL, respectively

(Fig. 5B). No significant changes in mitochondrial potential membrane health were observed at any tested concentration as well as in hFM-MSCs (Fig. 5C).

The effects of the scalar doses of BPS were then tested on hiPSCs: while very low dose (0.01 µM) sustained the cell proliferation, the higher doses (1 and 2 µM) were toxic, as evidenced by impedance values significantly lower than control after 48 h of treatment (Fig. 6A and Table 1). Also, the Ki67 expression was dramatically decreased by a 24-h exposure to the higher doses (Fig. 6B*)*, thus confirming the detrimental effect of 1- and 2-µM BPS on hiPSCs. The analysis was then completed by the study of the mitochondrial response: the image analysis of BPS-treated samples evidenced that this xenobiotic dramatically altered the mitochondrial health, as evidenced by the drop in the fluorescent intensity of the cells (Fig. 6C).

These results indicated that BPS interferes with the cell growth regulation at low doses, while at higher doses may exert a toxic effect; moreover, similarly to BPA, BPS deeply affects the mitochondrial membrane potential in hiPSCs.

Dose–Response Effects of PFOS on Perinatal Stem Cells and hiPSCs

PFOS induced effects similar to that evoked by BPA and BPS exposure. Low doses of PFOS, indeed, increased the hFM-MSC proliferation rate, at shorter (0.01 µM) or longer (0.1 µM) incubation timepoints; the 2-µM dosage promptly induced a decrease of cell number, but this effect was transitory and at 48-h impedance was significantly higher than control. No effect on impedance was recorded at 1 µM (Fig. 7A and Table 1). The early interference with proliferative machinery exerted by very low PFOS doses (0.01 µM) was also confirmed by the Ki67 immunostaining (Fig. 7B). On the other side, PFOS seemed to not affect the mitochondrial health of hFM-MSC, compared to the control condition as well. (Fig. 7C).

The hAFSCs similarly responded to low and medium doses (0.01–0.1 and 1 µM) of PFOS, as an increase of the proliferation rate as detected, but, by contrast, the highest concentration (2 µM) induced a significant drop of the impedance values (Fig. 8A and Table 1). These data were confirmed also by immunofluorescent analysis that showed an increase of Ki67^{+} cells after 24 h of treatment at all doses except for 2-µM PFOS that were statistically lower than the control. (Fig. 8B). No significant changes in mitochondrial potential membrane health were observed at any tested concentration as well as in hFM-MSCs (Fig. 8C).

By contrast, as observed with the other analyzed chemicals, only very low concentration (0.01 µM) of PFOS increased the hiPSCs proliferation rate, according to the impedance analysis at 48 h, while the exposure to 2-µM concentration determined a toxic effect, inducing a decrease in cell number and a drop in the percentage of Ki67 positive hiPSCs (Fig. 9A, 9B and Table 1). Again, the mitochondrial functionality was deeply affected after the treatment with all the PFOS concentration tested (Fig. 9C).

Dose–Response Effects of PFOA on Perinatal Stem Cells and hiPSCs

Low doses of PFOA (0.01–0.1 µM) increased the proliferation rate of hFM-MSCs, already after 6 h the administration of the pollutant; however, this effect appeared to be temporary, since at 48 h the impedance values were comparable to that of control. On the other side, the treatment with the highest concentration tested (2 µM) took at least 36-48 h to slightly, albeit significantly, increase the cell growth. Like PFOS, 1-µM PFOA did not induce any effects. The impedance data were consistent with the immunofluorescence against Ki67 that highlighted that only the 0.01-µM dose led to an increase of the positive cells after 24 h of treatment (Fig. 10A, B). Mitochondrial functionality was not altered by any PFOA concentration (Fig. 10C).

The proliferation rate of the hAFSCs were less affected by PFOA exposure, as only weak effect was observed at lowest concentration at late timepoints (Fig. 11A). Ki67^{+} immunostaining did not detect any significant difference compared to the control (Fig. 11B). Unlike in hFM-MSCs,
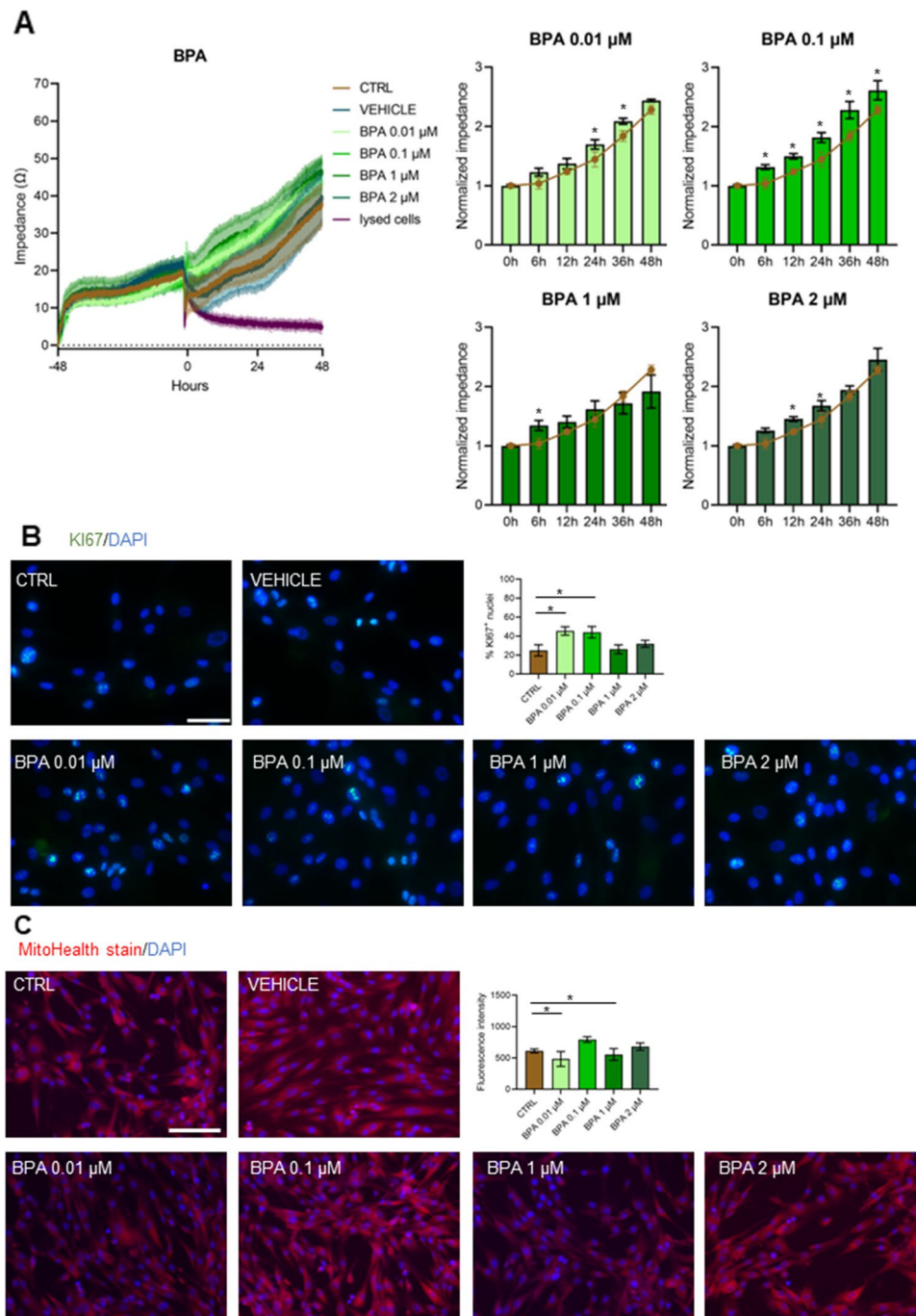
Fig. 2 Dose–response effects of BPA on hAFSCs. **A** On day 0 hAF-SCs were treated with different doses of BPA and the impedance values were monitored in real time up to 48 h. Green lines of increasing intensities, from pale to dark, represent the diverse BPA concentrations, as indicated. Cells not treated (brown line), treated only with the vehicle (dark blue line), or with lysing agents (purple line) represented the experimental controls. *Left panel*: absolute impedance values (expressed in ohms, Ω). Graph is representative of three different experiments. *Right Panel*: Normalized impedance values (Day 0 = 1) of Control (brown line) or BPA-treated samples (green histograms) at different concentrations, as indicated. Data are expressed as mean ± SD (n = 3, *p < 0.05 vs Control). **B** Immunocytochemical detection of Ki67 (green fluorescence) in hAFSC control cells and after 24-h

exposure to vehicle or different BPA concentrations. The nuclei were counterstained with DAPI (blue). Original magnification: 40x, scale bar 50 mm. Images are representative of 3 independent experiments. Graph on the right indicates the % of the positive nuclei in the different experimental conditions. Data are expressed as mean ± SD (n = 3, *p < 0.05 vs Control). **C** Immunocytochemical detection of mitochondria membrane potential (red fluorescence) in Control cells and after 24-h exposure to vehicle only or to different BPA concentrations. The nuclei were counterstained with DAPI (blue). Original magnification: 20×, scale bar 100 mm. Images are representative of 3 independent experiments. Graph indicates the fluorescent intensity (absolute values) in the different experimental conditions. Data are expressed as mean ± SD (n = 3, *p < 0.05 vs Control)
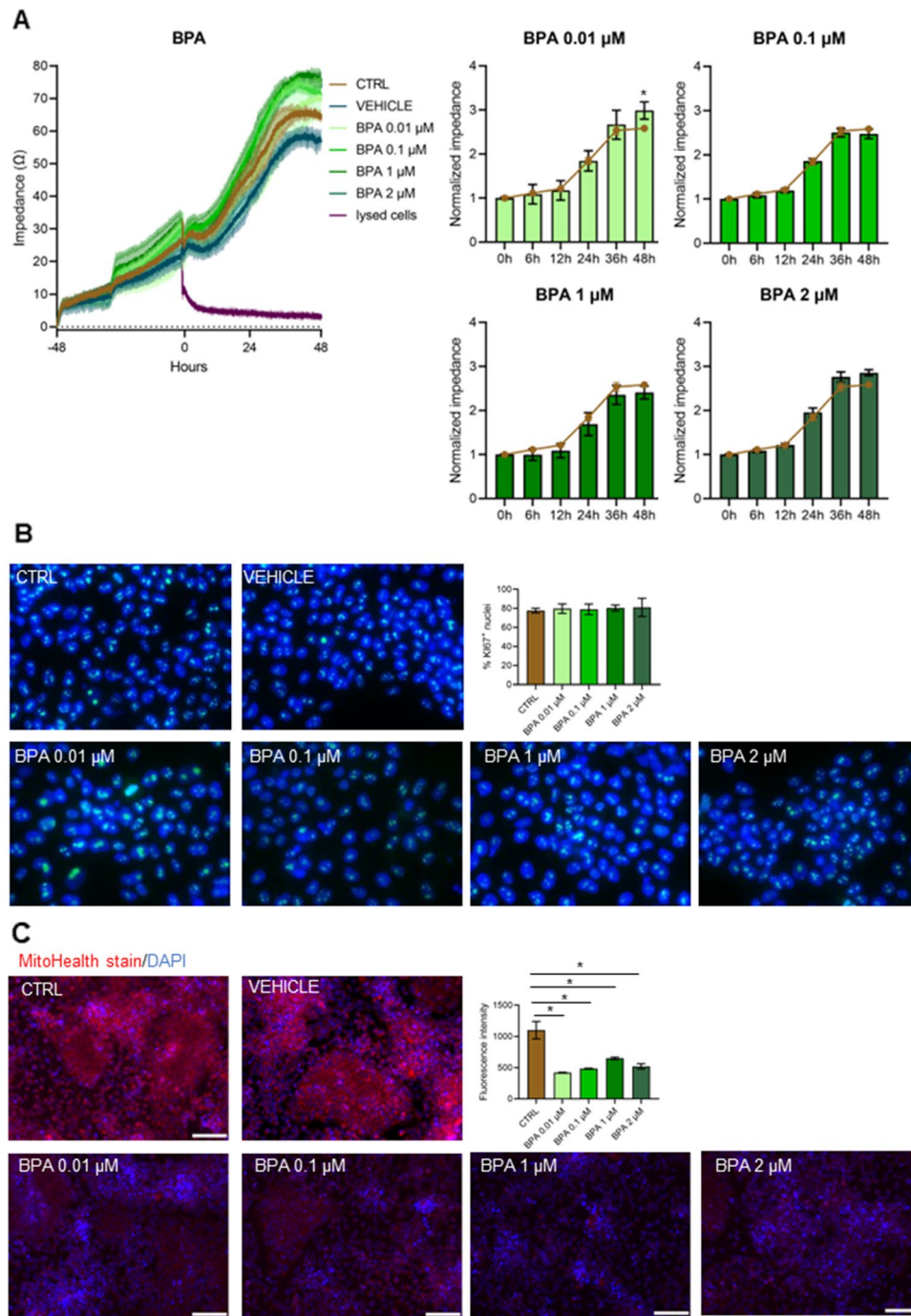
Fig. 3 Dose–response effects of BPA on hiPSCs. **A** On day 0 hiPSCs were treated with different doses of BPA and the impedance values were monitored in real time up to 48 h. Green lines of increasing intensities, from pale to dark, represent the diverse BPA concentrations, as indicated. Cells not treated (brown line), treated only with the vehicle (dark blue line), or with lysing agents (purple line) represented the experimental controls. *Left panel*: absolute impedance values (expressed in ohms, Ω). Graph is representative of three different experiments. *Right Panel*: Normalized impedance values (Day $0=1$) of Control (brown line) or BPA-treated samples (green histograms) at different concentrations, as indicated. Data are expressed as mean $\pm$ SD ($n=3$, *$p<0.05$ vs Control). **B** Immunocytochemical detection of Ki67 (green fluorescence) in hiPSC control cells and after 24-h exposure to vehicle or different BPA concentrations. The nuclei were counterstained with DAPI (blue). Original magnification: 40x, scale bar 50 mm. Images are representative of 3 independent experiments. Graph on the right indicates the % of the positive nuclei in the different experimental conditions. Data are expressed as mean $\pm$ SD ($n=3$, *$p<0.05$ vs Control). **C** Immunocytochemical detection of mitochondria membrane potential (red fluorescence) in Control cells and after 24-h exposure to vehicle only or to different BPA concentrations. The nuclei were counterstained with DAPI (blue). Original magnification: 20×, scale bar 100 mm. Images are representative of 3 independent experiments. Graph indicates the fluorescent intensity (absolute values) in the different experimental conditions. Data are expressed as mean $\pm$ SD ($n=3$, *$p<0.05$ vs Control)
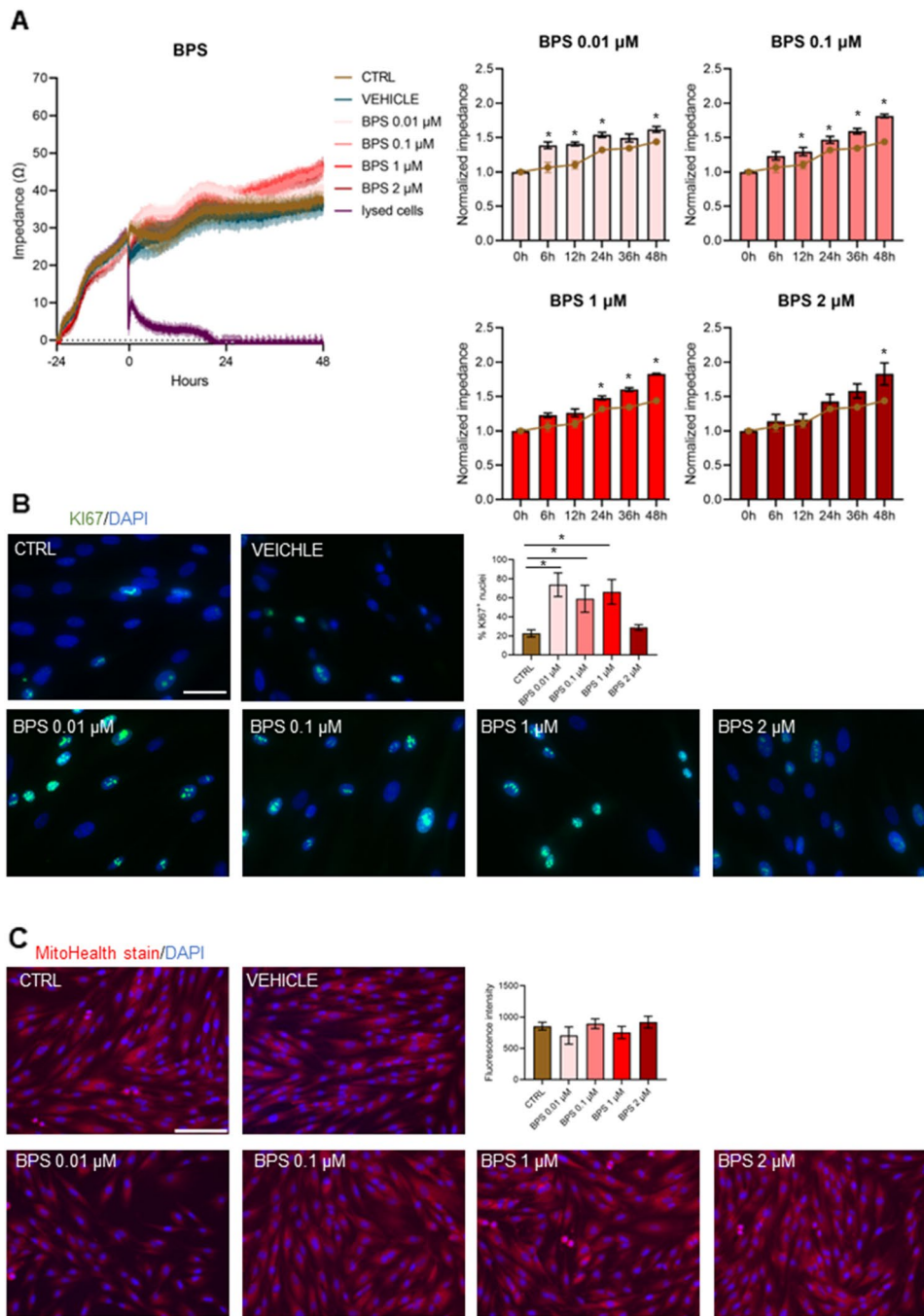
Fig. 4 Dose–response effects of BPS on hFM-MSCs. **A** On day 0 hFM-MSCs were treated with different doses of BPS and the impedance values were monitored in real time up to 48 h. Red lines of increasing intensities, from pale to dark, represent the diverse BPS concentrations, as indicated. Cells not treated (brown line), treated only with the vehicle (dark blue line), or with lysing agents (purple line) represented the experimental controls. *Left panel:* absolute impedance values (expressed in ohms, Ω). Graph is representative of three different experiments. *Right Panel:* Normalized impedance values (Day 0 = 1) of Control (brown line) or BPS-treated samples (red histograms) at different concentrations, as indicated. Data are expressed as mean ± SD ($n = 3$, *$p < 0.05$ vs Control). **B** Immunocytochemical detection of Ki67 (green fluorescence) in hFM-MSC control cells and after 24-h exposure to vehicle or different BPS concentrations. The nuclei were counterstained with DAPI (blue). Original magnification: 40x, scale bar 50 mm. Images are representative of 3 independent experiments. Graph on the right indicates the % of the positive nuclei in the different experimental conditions. Data are expressed as mean ± SD ($n = 3$, *$p < 0.05$ vs Control). **C** Immunocytochemical detection of mitochondria membrane potential (red fluorescence) in Control cells and after 24-h exposure to vehicle only or to different BPS concentrations. The nuclei were counterstained with DAPI (blue). Original magnification: 20×, scale bar 100 mm. Images are representative of 3 independent experiments. Graph indicates the fluorescent intensity (absolute values) in the different experimental conditions. Data are expressed as mean ± SD ($n = 3$, *$p < 0.05$ vs Control)
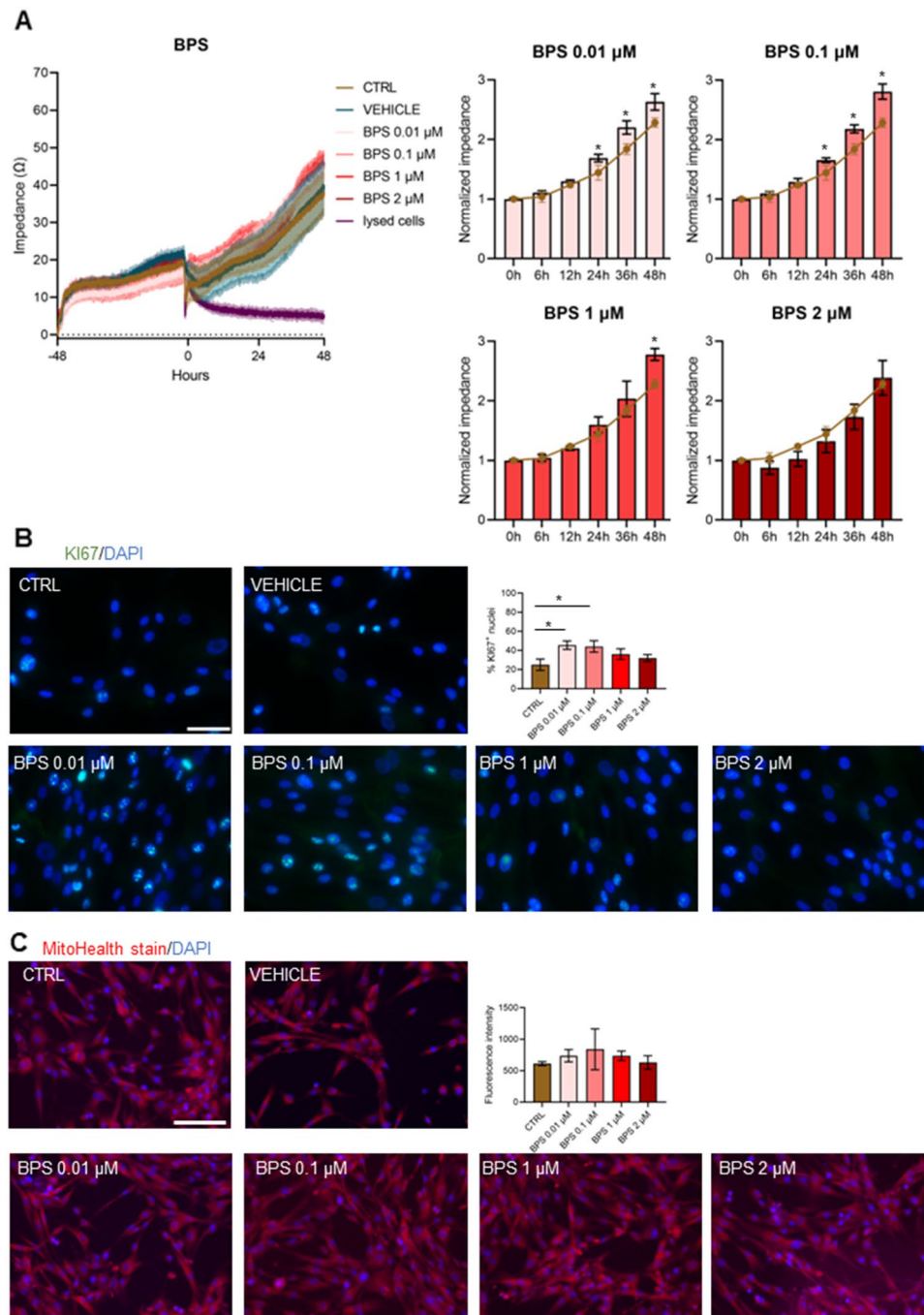
Fig. 5 Dose–response effects of BPS on hAFSCs. **A** On day 0 hAF-SCs were treated with different doses of BPS and the impedance values were monitored in real time up to 48 h. Red lines of increasing intensities, from pale to dark, represent the diverse BPS concentrations, as indicated. Cells not treated (brown line), treated only with the vehicle (dark blue line) or with lysing agents (purple line) represented the experimental controls. *Left panel*: absolute impedance values (expressed in ohms, Ω). Graph is representative of three different experiments. *Right Panel*: Normalized impedance values (Day 0=1) of Control (brown line) or BPS-treated samples (red histograms) at different concentrations, as indicated. Data are expressed as mean ± SD ($n=3$, *$p<0.05$ vs Control). **B** Immunocytochemical detection of Ki67 (green fluorescence) in hAFSC control cells and after 24-h

exposure to vehicle or different BPS concentrations. The nuclei were counterstained with DAPI (blue). Original magnification: 40x, scale bar 50 mm. Images are representative of 3 independent experiments. Graph on the right indicates the % of the positive nuclei in the different experimental conditions. Data are expressed as mean ± SD ($n=3$, *$p<0.05$ vs Control). **C** Immunocytochemical detection of mitochondria membrane potential (red fluorescence) in Control cells and after 24-h exposure to vehicle only or to different BPS concentrations. The nuclei were counterstained with DAPI (blue). Original magnification: 20×, scale bar 100 mm. Images are representative of 3 independent experiments. Graph indicates the fluorescent intensity (absolute values) in the different experimental conditions. Data are expressed as mean ± SD ($n=3$, *$p<0.05$ vs Control)
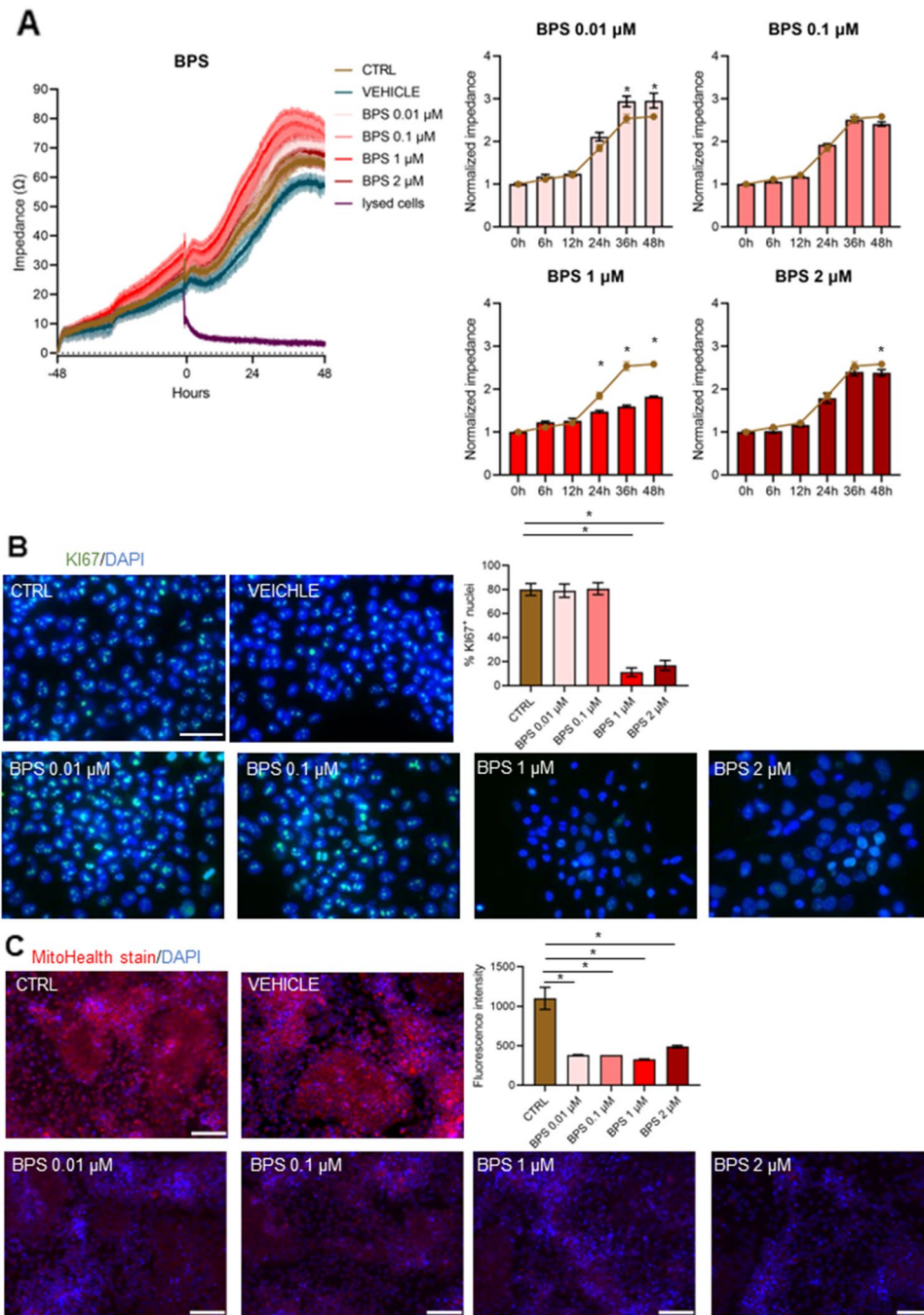
Fig. 6 Dose–response effects of BPS on hiPSCs. **A** On day 0 hiPSCs were treated with different doses of BPS and the impedance values were monitored in real time up to 48 h. Red lines of increasing intensities, from pale to dark, represent the diverse BPS concentrations, as indicated. Cells not treated (brown line), treated only with the vehicle (dark blue line), or with lysing agents (purple line) represented the experimental controls. *Left panel*: absolute impedance values (expressed in ohms, Ω). Graph is representative of three different experiments. *Right Panel*: Normalized impedance values (Day 0 = 1) of Control (brown line) or BPS-treated samples (red histograms) at different concentrations, as indicated. Data are expressed as mean ± SD ($n=3$, *$p < 0.05$ vs Control). **B** Immunocytochemical detection of Ki67 (green fluorescence) in hiPSC control cells and after 24-h

exposure to vehicle or different BPS concentrations. The nuclei were counterstained with DAPI (blue). Original magnification: 40×, scale bar 50 mm. Images are representative of 3 independent experiments. Graph on the right indicates the % of the positive nuclei in the different experimental conditions. Data are expressed as mean ± SD ($n=3$, *$p < 0.05$ vs Control). **C** Immunocytochemical detection of mitochondria membrane potential (red fluorescence) in Control cells and after 24-h exposure to vehicle only or to different BPS concentrations. The nuclei were counterstained with DAPI (blue). Original magnification: 20 ×, scale bar 100 mm. Images are representative of 3 independent experiments. Graph indicates the fluorescent intensity (absolute values) in the different experimental conditions. Data are expressed as mean ± SD ($n=3$, *$p < 0.05$ vs Control)
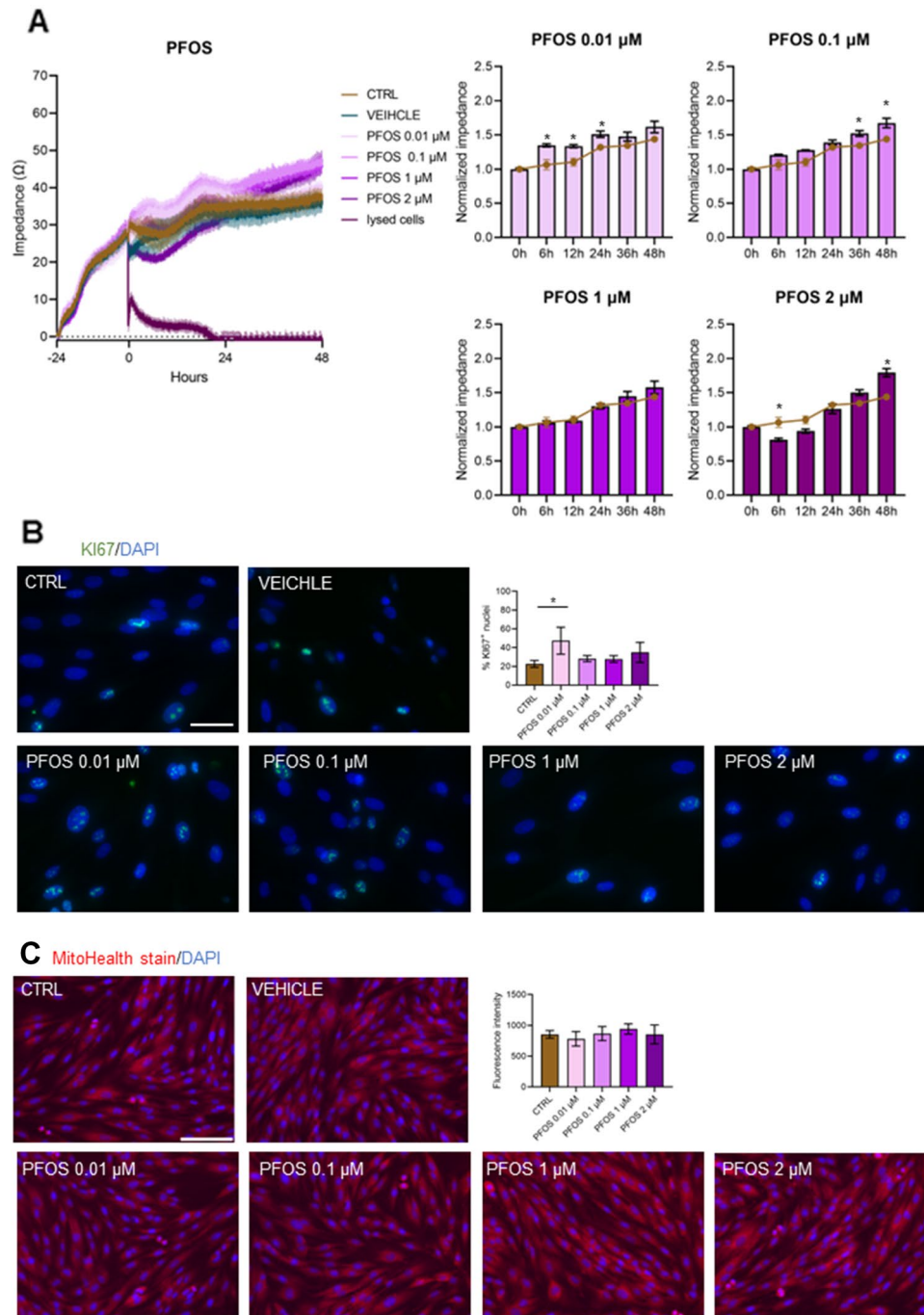
Fig. 7 Dose–response effects of PFOS on hFM-MSCs. **A** On day 0 hFM-MSCs were treated with different doses of PFOS and the impedance values were monitored in real time up to 48 h. Purple lines of increasing intensities, from pale to dark, represent the diverse PFOS concentrations, as indicated. Cells not treated (brown line), treated only with the vehicle (dark blue line), or with lysing agents (purple line) represented the experimental controls. *Left panel*: absolute impedance values (expressed in ohms, Ω). Graph is representative of three different experiments. *Right Panel*: Normalized impedance values (Day $0 = 1$) of Control (brown line) or PFOS-treated samples (purple histograms) at different concentrations, as indicated. Data are expressed as mean $\pm$ SD ($n = 3$, $* p < 0.05$ vs Control). **B** Immunocytochemical detection of Ki67 (green fluorescence) in hFM-MSC control cells and after 24-h exposure to vehicle or differ- ent PFOS concentrations. The nuclei were counterstained with DAPI (blue). Original magnification: 40×, scale bar 50 mm. Images are representative of 3 independent experiments. Graph on the right indicates the % of the positive nuclei in the different experimental conditions. Data are expressed as mean $\pm$ SD ($n = 3$, $*p < 0.05$ vs Control). **C** Immunocytochemical detection of mitochondria membrane potential (red fluorescence) in Control cells and after 24-h exposure to vehicle only or to different PFOS concentrations. The nuclei were counterstained with DAPI (blue). Original magnification: 20x, scale bar 100 mm. Images are representative of 3 independent experiments. Graph indicates the fluorescent intensity (absolute values) in the different experimental conditions. Data are expressed as mean $\pm$ SD ($n = 3$, $*p < 0.05$ vs Control)
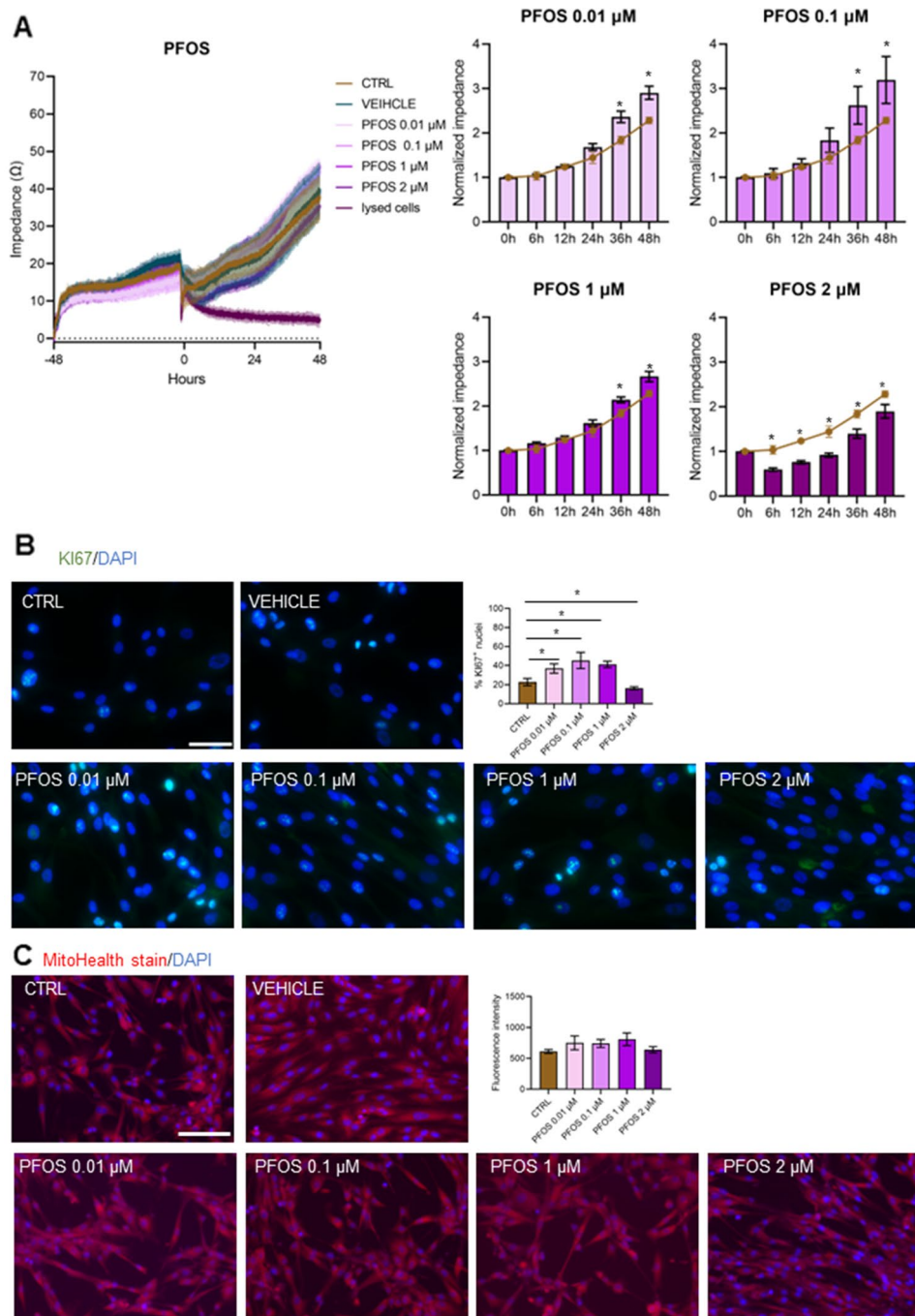
Fig. 8 Dose–response effects of PFOS on hAFSCs. **A** On day 0 hAF-SCs were treated with different doses of PFOS and the impedance values were monitored in real time up to 48 h. Purple lines of increasing intensities, from pale to dark, represent the diverse PFOS concentrations, as indicated. Cells not treated (brown line), treated only with the vehicle (dark blue line), or with lysing agents (purple line) represented the experimental controls. *Left panel*: absolute impedance values (expressed in ohms, Ω). Graph is representative of three different experiments. *Right Panel*: Normalized impedance values (Day 0 = 1) of Control (brown line) or PFOS-treated samples (purple histograms) at different concentrations, as indicated. Data are expressed as mean ± SD (n = 3, *p < 0.05 vs Control). **B** Immunocytochemical detection of Ki67 (green fluorescence) in hAFSC control cells and after 24-h

exposure to vehicle or different PFOS concentrations. The nuclei were counterstained with DAPI (blue). Original magnification: 40x, scale bar 50 mm. Images are representative of 3 independent experiments. Graph on the right indicates the % of the positive nuclei in the different experimental conditions. Data are expressed as mean ± SD (n = 3, *p < 0.05 vs Control). **C** Immunocytochemical detection of mitochondria membrane potential (red fluorescence) in Control cells and after 24-h exposure to vehicle only or to different PFOS concentrations. The nuclei were counterstained with DAPI (blue). Original magnification: 20x, scale bar 100 mm. Images are representative of 3 independent experiments. Graph indicates the fluorescent intensity (absolute values) in the different experimental conditions. Data are expressed as mean ± SD (n = 3, *p < 0.05 vs Control)
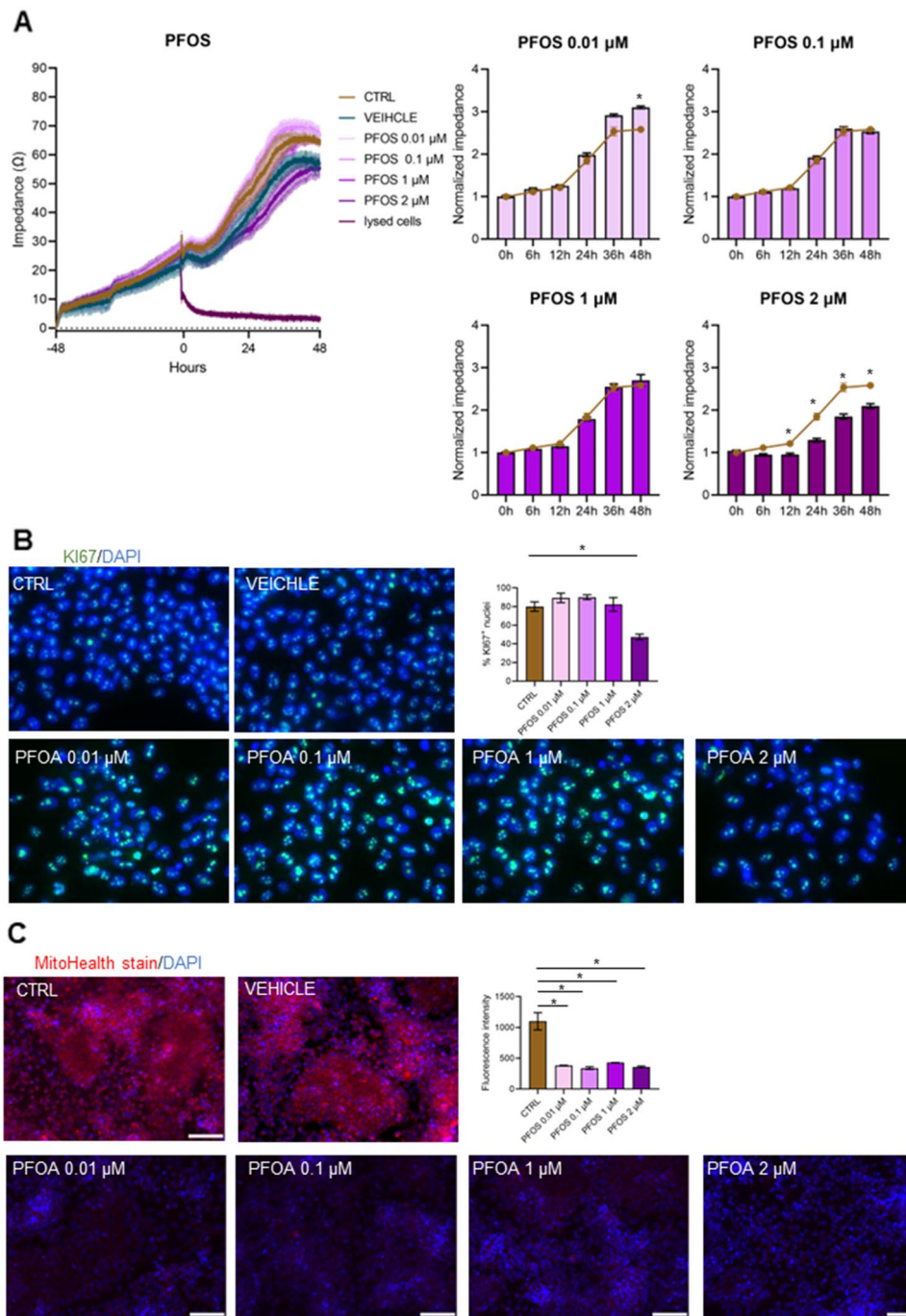
Fig. 9 Dose–response effects of PFOS on hiPSCs. **A** On day 0 hiP-SCs were treated with different doses of PFOS and the impedance values were monitored in real time up to 48 h. Purple lines of increasing intensities, from pale to dark, represent the diverse PFOS concentrations, as indicated. Cells not treated (brown line), treated only with the vehicle (dark blue line), or with lysing agents (purple line) represented the experimental controls. *Left panel*: absolute impedance values (expressed in ohms, Ω). Graph is representative of three different experiments. *Right Panel*: Normalized impedance values (Day 0 = 1) of Control (brown line) or PFOS-treated samples (purple histograms) at different concentrations, as indicated. Data are expressed as mean ± SD ($n = 3$, *$p < 0.05$ vs Control). **B** Immunocytochemical detection of Ki67 (green fluorescence) in hiPSC control cells and after 24-h exposure to vehicle or different PFOS concentrations. The nuclei were counterstained with DAPI (blue). Original magnification: 40x, scale bar 50 mm. Images are representative of 3 independent experiments. Graph on the right indicates the % of the positive nuclei in the different experimental conditions. Data are expressed as mean ± SD ($n = 3$, *$p < 0.05$ vs Control). **C** Immunocytochemical detection of mitochondria membrane potential (red fluorescence) in Control cells and after 24-h exposure to vehicle only or to different PFOS concentrations. The nuclei were counterstained with DAPI (blue). Original magnification: 20×, scale bar 100 mm. Images are representative of 3 independent experiments. Graph indicates the fluorescent intensity (absolute values) in the different experimental conditions. Data are expressed as mean ± SD ($n = 3$, *$p < 0.05$ vs Control)
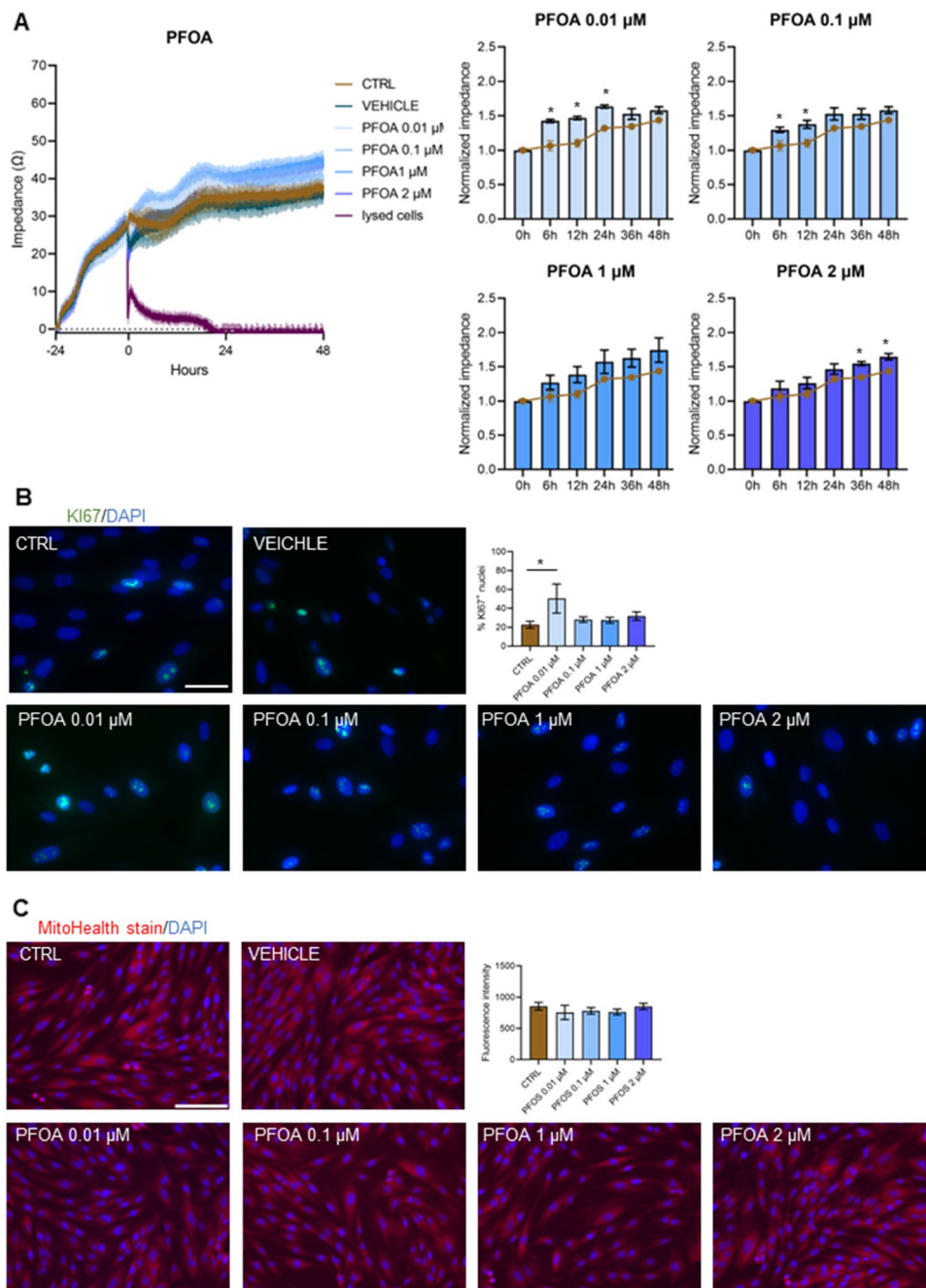
Fig. 10 Dose–response effects of PFOA on hFM-MSCs. **A** On day 0 hFM-MSCs were treated with different doses of PFOA and the impedance values were monitored in real time up to 48 h. Blue lines of increasing intensities, from pale to dark, represent the diverse PFOA concentrations, as indicated. Cells not treated (brown line), treated only with the vehicle (dark blue line), or with lysing agents (purple line) represented the experimental controls. *Left panel*: absolute impedance values (expressed in ohms, Ω). Graph is representative of three different experiments. *Right Panel*: Normalized impedance values (Day 0 = 1) of Control (brown line) or PFOA-treated samples (blue histograms) at different concentration, as indicated. Data are expressed as mean ± SD ($n = 3$, *$p < 0.05$ vs Control). **B** Immunocytochemical detection of Ki67 (green fluorescence) in hFM-MSC control cells and after 24-h exposure to vehicle or differ- ent PFOA concentrations. The nuclei were counterstained with DAPI (blue). Original magnification: 40x, scale bar 50 mm. Images are representative of 3 independent experiments. Graph on the right indi- cates the % of the positive nuclei in the different experimental con- ditions. Data are expressed as mean ± SD ($n = 3$, *$p < 0.05$ vs Con- trol). **C** Immunocytochemical detection of mitochondria membrane potential (red fluorescence) in Control cells and after 24-h exposure to vehicle only or to different PFOA concentrations. The nuclei were counterstained with DAPI (blue). Original magnification: 20x, scale bar 100 mm. Images are representative of 3 independent experiments. Graph indicates the fluorescent intensity (absolute values) in the dif- ferent experimental conditions. Data are expressed as mean ± SD ($n = 3$, *$p < 0.05$ vs Control)
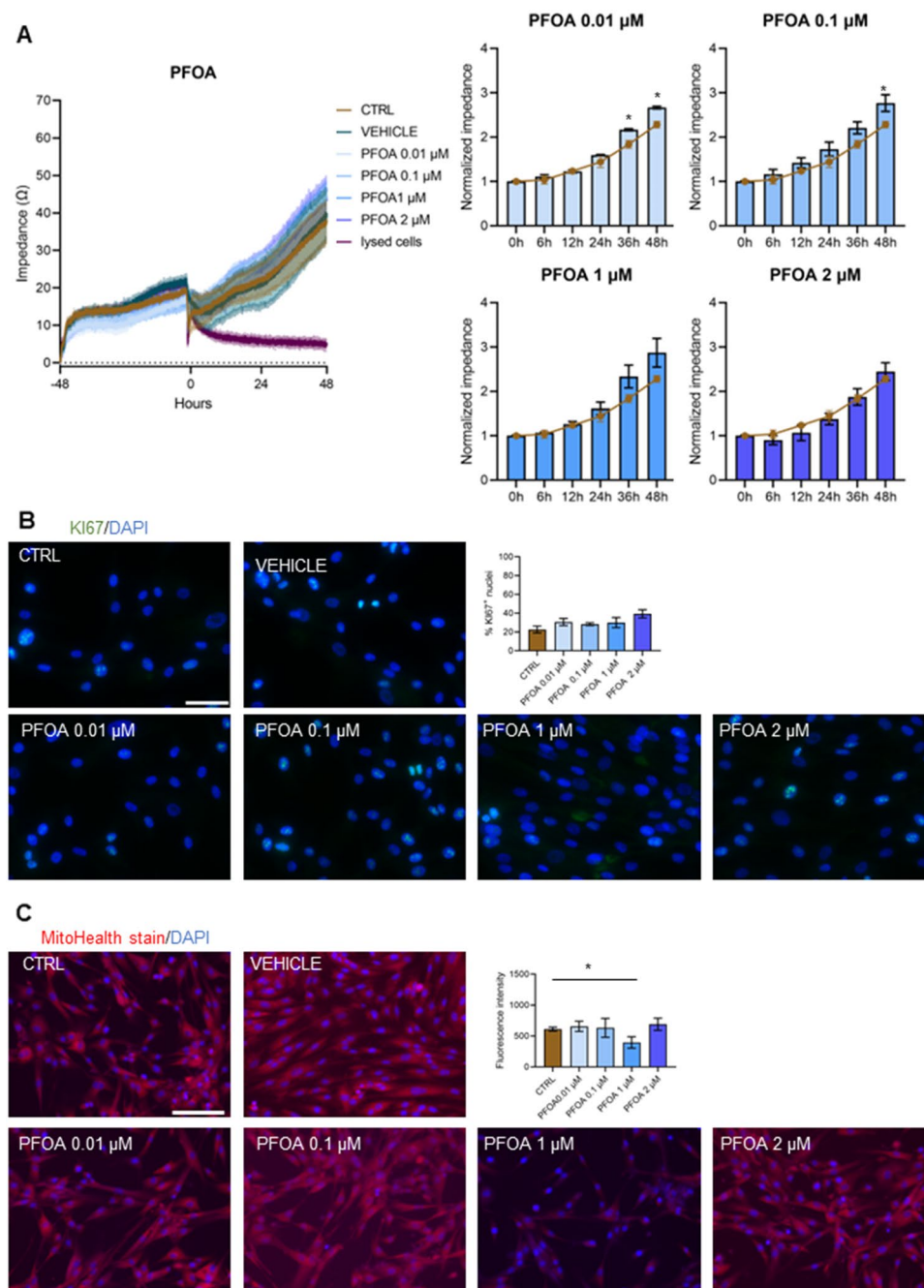
Fig. 11 Dose–response effects of PFOA on hAFSCs. **A** On day 0 hAFSCs were treated with different doses of PFOA and the impedance values were monitored in real time up to 48 h. Blue lines of increasing intensities, from pale to dark, represent the diverse PFOA concentrations, as indicated. Cells not treated (brown line), treated only with the vehicle (dark blue line), or with lysing agents (purple line) represented the experimental controls. *Left panel*: absolute impedance values (expressed in ohms, Ω). Graph is representative of three different experiments. *Right Panel*: Normalized impedance values (Day $0 = 1$) of Control (brown line) or PFOA-treated samples (blue histograms) at different concentrations, as indicated. Data are expressed as mean $\pm$ SD ($n = 3$, *$p < 0.05$ vs Control). **B** Immunocytochemical detection of Ki67 (green fluorescence) in hAFSC control cells and after 24-h exposure to vehicle or different PFOA concentrations. The nuclei were counterstained with DAPI (blue). Original magnification: 40x, scale bar 50 mm. Images are representative of 3 independent experiments. Graph on the right indicates the % of the positive nuclei in the different experimental conditions. Data are expressed as mean $\pm$ SD ($n = 3$, *$p < 0.05$ vs Control). **C** Immunocytochemical detection of mitochondria membrane potential (red fluorescence) in Control cells and after 24-h exposure to vehicle only or to different PFOA concentrations. The nuclei were counterstained with DAPI (blue). Original magnification: 20×, scale bar 100 mm. Images are representative of 3 independent experiments. Graph indicates the fluorescent intensity (absolute values) in the different experimental conditions. Data are expressed as mean $\pm$ SD ($n = 3$, *$p < 0.05$ vs Control)

intermediate PFOA concentration (1 μM) affected the mitochondrial membrane potential. (Fig. 11C).

Finally, as observed with the other analyzed chemical, according to the impedance analysis and Ki67 immunostaining (Fig. 12 A, B, Table 1), very low doses (0.01 μM) of PFOA boosted the cell proliferation of hiPSCs, while the other concentrations were not effective; however, PFOA induced an important mitotoxicity at all the concentration tested (Fig. 12C).

All the results are summarized in Table 2

Discussion

In this study we demonstrate that BPs and PFs can deeply affect stem cell biology, thus determining abnormal stem cell function and possible adverse effects on health at birth or later in adulthood; the main results of our study are that *i*. overall, PFs and BPs tend to drive perinatal stem cells toward proliferation; *ii*. hiPSCs responded to very low doses (0.01 μM) of BPs and PFs increasing their proliferation, while higher doses of BPS and PFOS were toxic; and *iii*. both BPs and PFs were mitotoxic for hiPSCs at all the tested concentration (Table 2).

BPs and PFs are compounds that act as EDs interfering with normal hormonal function. Since they can cross the blood–placenta barrier, it has been proposed that they may perturb the hormonal signaling in utero causing deregulation of the fetal development. Parental BPA accumulates in both fetal plasma and placental tissue (Schönfelder et al. 2002); BPS, which has been introduced as an alternative into many commercial products available on the market as "BPA-free," has been found in human placenta at concentrations higher than that detected in the maternal serum, suggesting an accumulation of this ED in the perinatal tissues (Pan et al. 2020). In addition, BPS exposure of pregnant women is associated with altered fetal growth patterns and changes in neonatal metabolic profile (Blaauwendraad et al. 2021). PFOS has been reported to induce morphological changes in mice placenta (Wan et al. 2020); similarly, in vitro studies on human placental cell lines reported an impairment of cell migration and angiogenesis (Li et al. 2021). In a model of human trophoblast, PFOA induced changes in the vascular 3D network structure (Poteser et al. 2020), while lead to a decrease of fetal survival and growth in mice (Jiang et al. 2020). All these studies prompted us to better define the role of BPs and PFs in human development. Since stem cells represent natural units of embryonic development, the study of the EDs effects on stem cells is pivotal to shed light on the health effects of prenatal exposure to these pollutants.

BPs and PFs exposure can affect the overall health of the pregnancy interfering with the finely orchestrated endocrine system, increasing maternal susceptibility to pregnancy complications, and predisposing the fetus to adverse health risks; indeed, the placenta is not an entirely effective barrier to maternal–fetal transfer of these xenobiotics, consequently, the bioaccumulation of these EDs in the fetus can be promoted, possibly compromising various metabolic and physiological processes and increasing the risk of developing pathologies during the post-natal period and later in adulthood (Developmental Origins of Health and Disease theory). Animal studies have recently demonstrated that prenatal exposure to low doses of BPA induces lasting epigenetic alterations, disrupts the sexually dimorphic gene expression patterns of estrogen receptors in mice brain (Kundakovic et al. 2013), and impacts on brain expression of several genes, including that related to mating, cell–cell signaling, behavior, neurodevelopment, neurogenesis, synapse formation, cognition, and learning behaviors (Henriksen et al. 2020). On the other hand, several studies have observed associations between PFs and thyroid hormones during pregnancy (Aimuzi et al. 2020), and it has been reported that these chemicals may disrupt androgenic and estrogenic pathways in pregnancy in a sex-dependent manner exerting androgenic effects in pregnancy (Rivera-Núñez et al. 2023).

While animal research studies frequently employ high exposure doses of EDs that do not mimic "real life," one strength of our study is that we tested a range BPs and PFs concentrations that resemble the xenobiotic levels detected in maternal and infant samples (Lorigo and Cairrao 2022; Rivera-Núñez, et al. 2023; Jin et al. 2020; Lauritzen et al. 2016). Moreover, in addition to the widely used immunostaining for the proliferation marker Ki67, we exploited the MEA biosensor technology on hiPSCs, hFM-MSCs, and hAFSCs that, thanks to the adherent nature of all these cells, provide a more sensitive and valuable assessment of the proliferation by measuring their impedance values: being this technique noninvasive and label-free, the dynamics of these changes can be monitored in real time. The study of the kinetic response is important because the analysis of a single time point may lead to incorrect results: for example, we observed that low doses of PFOS (0.01 uM) and PFOA (0.01 and 0.1 uM) promptly increased the proliferation of hFM-MSCs, while after 48 h of exposure, the impedance values were comparable to the control; a similar trend was observed in hAFSCs treated with BPA. On the other hand, we observed that hFM-MSCs were able to recover from the toxic effect promptly exerted by 2-μM PFOS. All these observations suggest that BFs and PFs interact in a complex way with the cell proliferative machinery; endocrine disruptors can affect proliferation in different ways. BPA shows a significant interaction on neural stem cell proliferation and differentiation in the rat via the Wnt/β-catenin signaling pathway (Tiwari et al. 2015), while PFOS disturbs cell proliferation by activating the glycogen synthase kinase-3β with
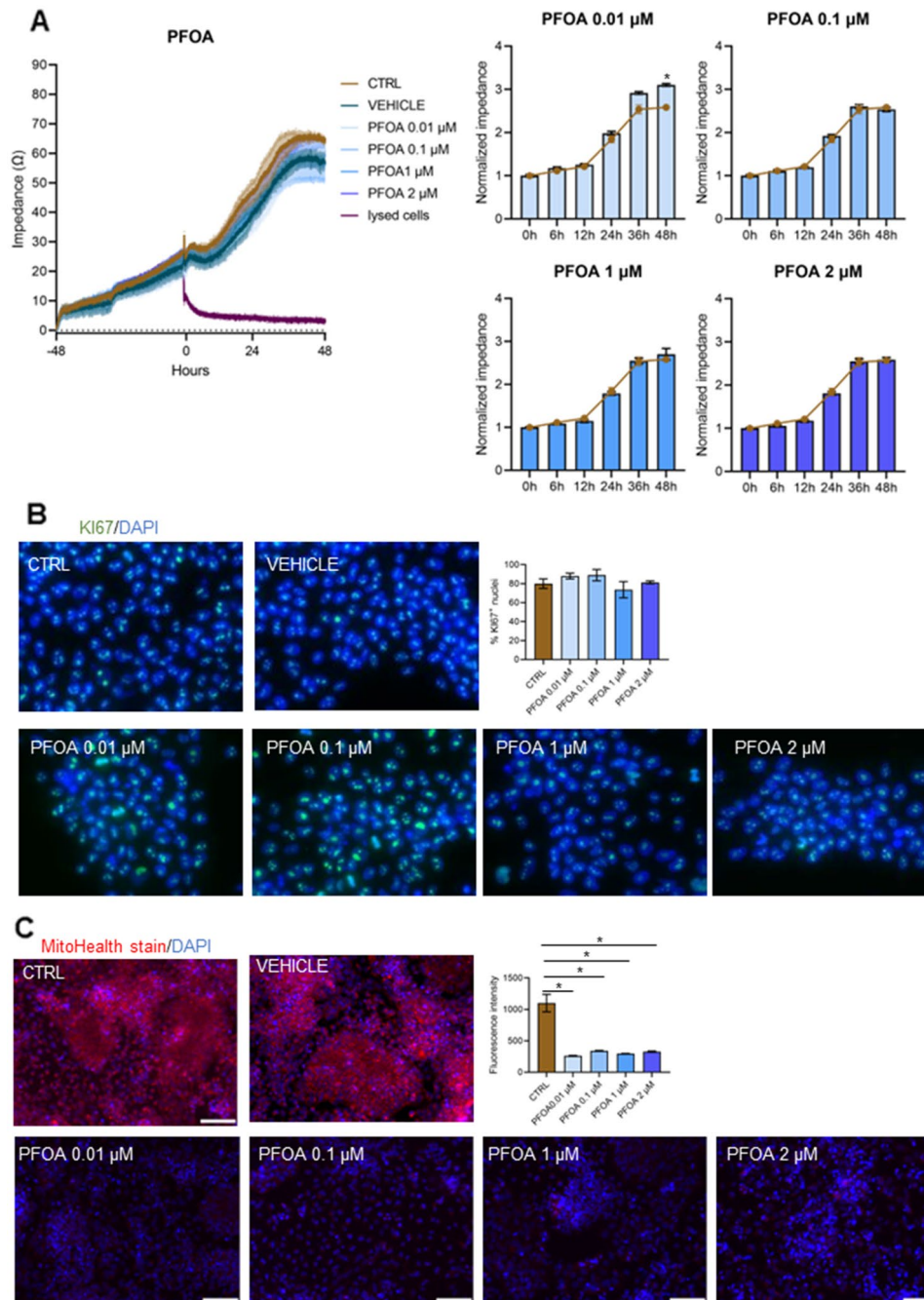
Fig. 12 Dose–response effects of PFOA on hiPSCs. **A** On day 0 hiP-SCs were treated with different doses of PFOA and the impedance values were monitored in real time up to 48 h. Blue lines of increasing intensities, from pale to dark, represent the diverse PFOA concentrations, as indicated. Cells not treated (brown line), treated only with the vehicle (dark blue line), or with lysing agents (purple line) represented the experimental controls. *Left panel*: absolute impedance values (expressed in ohms, Ω). Graph is representative of three different experiments. *Right Panel*: Normalized impedance values (Day 0 = 1) of Control (brown line) or PFOA-treated samples (blue histograms) at different concentrations, as indicated. Data are expressed as mean $\pm$ SD ($n = 3$, $*p < 0.05$ vs Control). **B** Immunocytochemical detection of Ki67 (green fluorescence) in hiPSC control cells and after 24-h exposure to vehicle or different PFOA concentrations. The nuclei were counterstained with DAPI (blue). Original magnification: 40x, scale bar 50 mm. Images are representative of 3 independent experiments. Graph on the right indicates the % of the positive nuclei in the different experimental conditions. Data are expressed as mean $\pm$ SD ($n = 3$, $*p < 0.05$ vs Control). **C** Immunocytochemical detection of mitochondria membrane potential (red fluorescence) in Control cells and after 24-h exposure to vehicle only or to different PFOA concentrations. The nuclei were counterstained with DAPI (blue). Original magnification: 20×, scale bar 100 mm. Images are representative of 3 independent experiments. Graph indicates the fluorescent intensity (absolute values) in the different experimental conditions. Data are expressed as mean $\pm$ SD ($n = 3$, $*p < 0.05$ vs Control)

Table 2 Effects of 48-h exposure BPs and PFs at different doses on the proliferation and on mitochondrial membrane potential of perinatal stem cells and hiPSCs

Cell type		hFM-MSCs		hAFSCs		hiPSCs	
		Proliferation	Mitotoxicity	Proliferation	Mitotoxicity	Proliferation	Mitotoxicity
BPA	0.01 uM	+	+	No effect	+	+	+
	0.1 uM	+	No effect	+	No effect	No effect	+
	1 uM	+	+	No effect	+	No effect	+
	2 uM	+	+	No effect	No effect	No effect	+
BPS	0.01 uM	+	No effect	+	No effect	+	+
	0.1 uM	+	No effect	+	No effect	No effect	+
	1 uM	+	No effect	+	No effect	–	+
	2 uM	+	No effect	No effect	No effect	–	+
PFOS	0.01 uM	No effect	No effect	+	No effect	+	+
	0.1 uM	+	No effect	+	No effect	No effect	+
	1 uM	No effect	No effect	+	No effect	No effect	+
	2 uM	+	No effect	-	No effect	–	+
PFOA	0.01 uM	No effect	No effect	+	No effect	+	+
	0.1 uM	No effect	No effect	+	No effect	No effect	+
	1 uM	No effect	No effect	No effect	+	No effect	+
	2 uM	+	No effect	No effect	No effect	No effect	+

The table summarizes the results obtained from scalar doses of BPA, BPS, PFOS, and PFOA on the proliferation (measured as impedance values) and on mitochondrial membrane potential (measured as fluorescent intensity of the MitoHealth Staining) of perinatal stem cells and hiPSCs. + and –: significant increased or decreased fold change vs CTRL, respectively, $p < 0.05$

resultant downregulation of cellular β-catenin (Dong et al. 2016); Pierozan et al. have recently described that PFOS and PFOA deregulate cyclin D1, CDK6, p21, p53, p27, ERK 1/2, and p38 in breast epithelial cells and that the cell cycle alteration persists in unexposed daughter cells after one and two passages (Pierozan et al. 2020); however, the EDs doses utilized in this study were above the normal range of exposure (10-μM PFOS and 100-μM PFOA), and the overall mechanisms through which BPs and PFs at lower concentration (similar to the current daily exposure of humans) may alter regulatory cell cycle proteins need to be clarified.

By reason of ethical and methodological issues, developmental toxicity studies are usually conducted in animal models, but due to the inter-species differences in the hormonal involvement during development, current animal-based testing methods can be considered neither specific nor sensitive enough to predict the effects of the in utero exposure to BPs and PFs. Up to date, indeed, the implications of human intrauterine exposure were easily extrapolated from their interferent activities, and our knowledge on antenatal exposure of human stem cells to BPs and PFs remains limited and controversial (Annab et al. 2012). In vitro models that mimic the in utero situation would allow more in-depth analysis of physiological processes essential for normal human development, such as the regulation of the self-renewal and differentiation of stem cells. In this study we exploited different human stem cells: hiPSCs, that are similar to embryonic stem cells that constitute the inner cells mass of the blastocyst and then may be considered as an "in vitro" model of developing embryos, and perinatal stem cells (hFM-MSCs and hAFSCs) that, isolated from human fetal annexes, allow the study of the "environment" in which the embryo is developing, whose alterations can affect fetal health. By means of this approach, we demonstrated that BPs and PFs disturb, even if at different extents and with diverse sensitivity, both the human embryonic-like cells (hiPSCs) and the fetal annexes-derived stem cells (hFM-MSCs and hAFSCs), by interfering with pivotal aspects of stem cell biology, such as the mitochondrial activity and proliferation rate. These observations offer new perspectives for understanding the fundamental mechanisms underlying the EDs effects on stem cells.

Profita and coll have recently evidenced that BPA and BPS, already at sub-nanomolar concentrations, affect the proliferation of human trophoblast cell line through ER/MAPK-mediated processes (Profita et al. 2021). Our results confirm and extend these data, evidencing that, albeit to a varying degree, BPs and PFs modify the proliferation of the stem cells present in the placenta, in the amniotic fluid and also of the embryonic-like stem cells. Like other EDs, BPs and PFs displayed non-linear dose–response curves, and the low and intermediate concentrations appear to be more effective than the higher. Interestingly, hiPSCs were particularly sensitive to very low doses (0.01 uM) of the

BPs and PFs that induced a significative proliferative surge in, while higher concentrations were not effective (BPA and PFOA) or toxic (BPS and PFOS). Collectively, these data evidence that BPs and PFs can perturb stem cell biology also at low concentrations. It is evident that the proliferative characteristics of the stem cells, which include the ability to both self-renew and differentiate by asymmetric divisions, must be strictly regulated especially during the critical window of the development, when interferences in the cell cycle regulation of stem cells may induce permanent alterations to developing tissues and organs. It is also worth noting that in hiPSCs intermediate concentration (0.1 μM and 1 μM) BPS appear to be more toxic than the same concentration of BPA: based on this result, the replacement of BPA with BPS in several daily objects does not represent a safer choice for human health.

Exposure to BPs and PFs results in oxidative stress and alterations of mitochondrial biogenesis, mitochondrial membrane potential (MMP) decline, and mitophagy (Nayak et al. 2022) (Zhou et al. 2022). It is well known that mitochondria are structurally complex organelles that provide energy to the cells by synthesizing ATP and have important roles in several metabolic pathways and in ROS production; regulating the cytosolic Ca^{2+} concentration, mitochondria also modulate cell signaling pathways associated with cell proliferation, differentiation, cell cycle progression, and apoptosis (Osellame et al. 2012). All of these functions may be significant in aging and/or disease (Bisaccia et al. 2021). The integrity of MMP is essential for maintaining mitochondrial structure, function, and metabolism, and therefore, its depolarization is a good indicator of mitochondrial dysfunction. In this study, we evaluated the BPs and PFs effects on MMP using the MitoHealth assay, a fluorescent live stain that accumulates in mitochondria proportionally to the MMP. Our data evidenced that, even though mitochondria of perinatal stem cells were not affected by the treatments, BPs and PFs exerted an important mitotoxic activity in hiPSCs. The mitochondrial number, morphology, ultrastructure, and distribution in hiPSCs are remarkably similar to those of ESCs; hiPSCs exhibit an elevated rate of proliferation and a significant part of cellular energy is expended to sustain the cell growth and at the same time to preserve their specific features of self-renewal and potency (Bukowiecki et al. 2014). In this scenario, the MMP modifications induced in hiPSCs by BPs and PFs are particularly significant. Accumulating evidence suggests, indeed, that mitochondrial function and integrity affect stem cell viability, proliferative and differential potential, and lifespan (Parker et al. 2009). Although the exact molecular mechanism leading BPs and PFs to MMP impairment and consequently, their effect on mitochondrial function requires detailed investigation, previous data have evidenced that endocrine disruptors can interfere with mitochondrial function through different pathways. PFs can accumulate inside the of eukaryotic membranes altering ion permeability and thus inducing changes in MMP (Qiao et al. 2019; Kleszczyński and Składanowski 2009) and PFOS induced mitochondrial dysfunction via blocking autophagy-lysosome degradation (Liu et al. 2020b); experiments performed on neuronal cells show that BPA affects key regulatory proteins of mitochondrial import pathways (PGC1α and TFAM) and mitochondrial biogenesis (GFER); moreover, the BPA-dependent change in MMP triggers apoptosis by inducing the cytochrome c translocation into the cytosol and reduce the antioxidants superoxide dismutase and catalase (Goyal et al. 2021). Given the diverse sensibility of the different cell populations, understanding the mechanisms through which BPs and PFs affect the MMP of stem cells may be critical in defying their toxic activity and may significantly improve research on EDs and pollutants.

In conclusion, our data suggest that antenatal exposure to BPs and PFs, also at very low concentrations, may modify the biological characteristics of stem cells present in both the developing fetus and the fetal annexes, thus perturbing normal human development. Since health risk assessment for these xenobiotics is complicated by several factors, including the wide disparity observed in the dose–response relationships reported in animal toxicity bioassays (Perez et al. 2023), in vitro studies may represent a useful tool in toxicological studies: indeed, data from these cellular models related to human embryo development can help us to better understand what effects BPs and PFs may have on human health and to establish more precisely which mechanisms are associated with the pathophysiology of the diseases.

Declarations

References

Abrantes-Soares F, Lorigo M, Cairrao, E (2022) Effects of BPA substitutes on the prenatal and cardiovascular systems. Crit Rev Toxicol 52(6):469–498. https://doi.org/10.1080/10408444.2022.2142514

Aimuzi R et al (2020) Perfluoroalkyl and polyfluroalkyl substances and maternal thyroid hormones in early pregnancy. Environ Pollut 264:114557. https://doi.org/10.1016/j.envpol.2020.114557

Annab LA et al (2012) Differential responses to retinoic acid and endocrine disruptor compounds of subpopulations within human embryonic stem cell lines. Differentiation 84(4):330–343. https://doi.org/10.1016/j.diff.2012.07.006

Antonucci I et al (2014) Human second trimester amniotic fluid cells are able to create embryoid body-like structures in vitro and to show typical expression profiles of embryonic and primordial germ cells. Cell Trans 23(12):1501–1515. https://doi.org/10.3727/096368914X678553

Behr A-C, Lichtenstein D, Braeuning A, Lampen A, Buhrke T (2018) Perfluoroalkylated substances (PFAS) affect neither estrogen and androgen receptor activity nor steroidogenesis in human cells in vitro. Toxicol Lett 291:51–60. https://doi.org/10.1016/j.toxlet.2018.03.029

Benjamin S, Masai E, Kamimura N, Takahashi K, Anderson RC, Faisal PA (2017) Phthalates impact human health: epidemiological evidences and plausible mechanism of action. J Hazard Mater 340:360–383. https://doi.org/10.1016/j.jhazmat.2017.06.036

Bisaccia G, Ricci F, Gallina S, Di Baldassarre A, Ghinassi, B (2021) Mitochondrial dysfunction and heart disease: critical appraisal of an overlooked association. Int J Mol Sci 22(2):614. https://doi.org/10.3390/ijms22020614

Blaauwendraad SM et al (2021) Associations of maternal bisphenol urine concentrations during pregnancy with neonatal metabolomic profiles. Metabolomics 17(9):84. https://doi.org/10.1007/s11306-021-01836-w

Bukowiecki R, Adjaye J, Prigione A (2014) Mitochondrial Function in Pluripotent Stem Cells and Cellular Reprogramming. Gerontology 60(2):174–182. https://doi.org/10.1159/000355050

Coperchini F et al (2021) Thyroid disrupting effects of old and new generation PFAS. Front. Endocrinol. 11:612320. https://doi.org/10.3389/fendo.2020.612320

Di Baldassarre A, Cimetta E, Bollini S, Gaggi G, Ghinassi, B (2018) Human-induced pluripotent stem cell technology and cardiomyocyte generation: progress and clinical applications. Cells. https://doi.org/10.3390/cells7060048

Di Credico A et al (2021) Real-time monitoring of levetiracetam effect on the electrophysiology of an heterogenous human iPSC-derived neuronal cell culture using microelectrode array technology. Biosensors 11(11):450. https://doi.org/10.3390/bios11110450

Di Giacomo V et al (2005) Expression of signal transduction proteins during the differentiation of primary human erythroblasts. J Cell Physiol 202(3):831–838. https://doi.org/10.1002/jcp.20179

Dong X, Yang J, Nie X, Xiao J, Jiang S (2016) Perfluorooctane sulfonate (PFOS) impairs the proliferation of C17. 2 neural stem cells via the downregulation of GSK-3β/β-catenin signaling. J Appl Toxicol 36(12):1591–1598. https://doi.org/10.1002/jat.3320

Du G et al (2013) Perfluorooctane sulfonate (PFOS) affects hormone receptor activity, steroidogenesis, and expression of endocrine-related genes in vitro and in vivo. Environ Toxicol Chem 32(2):353–360. https://doi.org/10.1002/etc.2034

Fenichel P, Chevalier N, Brucker-Davis F (2013) Bisphenol A: an endocrine and metabolic disruptor. Ann Endocrinol 74(3):211–220. https://doi.org/10.1016/j.ando.2013.04.002

Gaggi G, Izzicupo P, Di Credico A, Sancilio S, Di Baldassarre A, Ghinassi B (2019) Spare parts from discarded materials: fetal annexes in regenerative medicine. Int J Mol Sci. https://doi.org/10.3390/ijms20071573

Gaggi G et al (2020) Epigenetic features of human perinatal stem cells redefine their stemness potential. Cells. https://doi.org/10.3390/cells9051304

Gaggi G et al (2020) Human mesenchymal stromal cells unveil an unexpected differentiation potential toward the dopaminergic neuronal lineage. Int J Mol Sci. https://doi.org/10.3390/ijms21186589

Gaggi G, Di Credico A, Izzicupo P, Iannetti G, Di Baldassarre A, Ghinassi B (2021) Chemical and biological molecules involved in differentiation, maturation, and survival of dopaminergic neurons in health and parkinson's disease: physiological aspects and clinical implications. Biomedicines 9(7):754. https://doi.org/10.3390/biomedicines9070754

Gaggi G et al (2022) Human fetal membrane-mesenchymal stromal cells generate functional spinal motor neurons in vitro. iScience 25(10):105197. https://doi.org/10.1016/j.isci.2022.105197

Gaggi G, Di Credico A, Guarnieri S, Mariggiò MA, Di Baldassarre A, Ghinassi B (2022) Human mesenchymal amniotic fluid stem cells reveal an unexpected neuronal potential differentiating into functional spinal motor neurons Front. Cell Dev. Biol 10:936990. https://doi.org/10.3389/fcell.2022.936990

Ghassabian A, Vandenberg L, Kannan K, Trasande L (2022) Endocrine-disrupting chemicals and child health. Annu Rev Pharmacol Toxicol 62(1):573–594. https://doi.org/10.1146/annurev-pharmtox-021921-093352

Gore AC et al (2015) Executive summary to EDC-2: the endocrine society's second scientific statement on endocrine-disrupting chemicals. Endocr Rev 36(6):593–602. https://doi.org/10.1210/er.2015-1093

Goyal S et al (2021) Bisphenol-A inhibits mitochondrial biogenesis via impairment of GFER mediated mitochondrial protein import in the rat brain hippocampus. NeuroToxicology 85:18–32. https://doi.org/10.1016/j.neuro.2021.04.001

Henriksen AD, Andrade A, Harris EP, Rissman EF, Wolstenholme, JT (2020) Bisphenol A exposure in utero disrupts hypothalamic gene expression particularly genes suspected in autism spectrum disorders and neuron and hormone signaling. Int J Mol Sci 21(9):3129. https://doi.org/10.3390/ijms21093129

Hill CE, Myers JP, Vandenberg LN (2018) Nonmonotonic dose-response curves occur in dose ranges that are relevant to regulatory decision-making. Dose-Response 16(3):155932581879828. https://doi.org/10.1177/1559325818798282

Hulme CH et al (2018) Identification of the functional pathways altered by placental cell exposure to high glucose: lessons from the transcript and metabolite interactome. Sci Rep 8(1):5270. https://doi.org/10.1038/s41598-018-22535-y

Jiang W et al (2020) Gestational perfluorooctanoic acid exposure inhibits placental development by dysregulation of labyrinth vessels and uNK cells and apoptosis in mice. Front Physiol 11:51. https://doi.org/10.3389/fphys.2020.00051

Jin H et al (2020) Bisphenol analogue concentrations in human breast milk and their associations with postnatal infant growth. Environ Pollut 259:113779. https://doi.org/10.1016/j.envpol.2019.113779

Kleszczyński K, Składanowski AC (2009) Mechanism of cytotoxic action of perfluorinated acids. Toxicol Appl Pharmacol 3(234):300–5

Kundakovic M et al (2013) Sex-specific epigenetic disruption and behavioral changes following low-dose in utero bisphenol A exposure. Proc Natl Acad Sci 110(24):9956–9961. https://doi.org/10.1073/pnas.1214056110

Lau C et al (2006) Effects of perfluorooctanoic acid exposure during pregnancy in the mouse. Toxicol Sci 90(2):510–518. https://doi.org/10.1093/toxsci/kfj105

Lauritzen HB et al (2016) Factors associated with maternal serum levels of perfluoroalkyl substances and organochlorines: a descriptive study of parous women in Norway and Sweden. PLoS One 11(11):e0166127. https://doi.org/10.1371/journal.pone.0166127

Li Y et al (2018) Differential *in Vitro* biological action, coregulator interactions, and molecular dynamic analysis of bisphenol A (BPA), BPAF, and BPS ligand–ERα complexes. Environ Health Perspect 126(1):017012. https://doi.org/10.1289/EHP2505

Li J, Cao H, Feng H, Xue Q, Zhang A, Fu J (2020) Evaluation of the estrogenic/antiestrogenic activities of perfluoroalkyl substances and their interactions with the human estrogen receptor by combining *In Vitro* assays and *in silico* modeling. Environ Sci Technol 54(22):14514–14524. https://doi.org/10.1021/acs.est.0c03468

Li J, Quan X, Lei S, Huang Z, Wang Q, Xu P (2021) PFOS inhibited normal functional development of placenta Cells via PPARγ signaling. Biomedicines 9(6):677. https://doi.org/10.3390/biomedicines9060677

Liu Y, Li A, Buchanan S, Liu W (2020) Exposure characteristics for congeners, isomers, and enantiomers of perfluoroalkyl substances in mothers and infants. Environ Int 144:106012. https://doi.org/10.1016/j.envint.2020.106012

Liu D, Liu N-Y, Chen L-T, Shao Y, Shi X-M, Zhu D-Y (2020) Perfluorooctane sulfonate induced toxicity in embryonic stem cell-derived cardiomyocytes via inhibiting autophagy-lysosome pathway. Toxicol. In Vitro 69:104988. https://doi.org/10.1016/j.tiv.2020.104988

Lo B, Parham L (2009) Ethical issues in stem cell research. Endocr Rev 30(3):204–213. https://doi.org/10.1210/er.2008-0031

Lorigo M, Cairrao E (2022) Fetoplacental vasculature as a model to study human cardiovascular endocrine disruption. Mol Aspects Med. 87:101054. https://doi.org/10.1016/j.mam.2021.101054

Napso T et al (2021) Placental secretome characterization identifies candidates for pregnancy complications». Commun Biol 4(1):701. https://doi.org/10.1038/s42003-021-02214-x

Nayak D et al (2022) Impact of bisphenol a on structure and function of mitochondria: a critical review. Rev Environ Contam Toxicol 260(1):10. https://doi.org/10.1007/s44169-022-00011-z

Osellame LD, Blacker TS, e M. R. Duchen, (2012) Cellular and molecular mechanisms of mitochondrial function. Best Pract Res Clin Endocrinol Metab 26(6):711–723. https://doi.org/10.1016/j.beem.2012.05.003

Pan Y et al (2020) Occurrence and maternal transfer of multiple bisphenols, including an emerging derivative with unexpectedly high concentrations, in the human maternal–fetal–placental unit. Environ Sci Technol 54(6):3476–3486. https://doi.org/10.1021/acs.est.0c00206

Parker GC, Acsadi G, Brenner CA (2009) Mitochondria: determinants of Stem Cell Fate ? Stem Cells Dev 18(6):803–806. https://doi.org/10.1089/scd.2009.1806.edi

Parrotta E et al (2017) Two sides of the same coin? Unraveling subtle differences between human embryonic and induced pluripotent stem cells by Raman spectroscopy. Stem Cell Res Ther 8(1):271. https://doi.org/10.1186/s13287-017-0720-1

Perez A, Lumpkin M, Kornberg T, Schmidt A (2023) Critical endpoints of PFOA and PFOS exposure for regulatory risk assessment in drinking water: parameter choices impacting estimates of safe exposure levels. Regul Toxicol Pharmacol 138:105323. https://doi.org/10.1016/j.yrtph.2022.105323

Peterson AK et al (2022) Prenatal perfluorooctanoic acid (PFOA) exposure is associated with lower infant birthweight within the MADRES pregnancy cohort. Front Epidemiol 2:934715. https://doi.org/10.3389/fepid.2022.934715

Pierozan P, Cattani D, Karlsson O (2020) Perfluorooctane sulfonate (PFOS) and perfluorooctanoic acid (PFOA) induce epigenetic alterations and promote human breast cell carcinogenesis in vitro. Arch Toxicol 94:3893–906. https://doi.org/10.1007/s00204-020-02848-6

Poteser M, Hutter H-P, Moshammer H, Weitensfelder, L (2020) Perfluoroctanoic acid (PFOA) enhances NOTCH-signaling in an angiogenesis model of placental trophoblast cells. Int J Hyg Environ Health 229:113566. https://doi.org/10.1016/j.ijheh.2020.113566

Profita M, Fabbri E, Spisni E, Valbonesi P (2021) Comparing effects and action mechanisms of BPA and BPS on HTR-8/SVneo placental cells Biol. Reprod. 105(5):1355–1364. https://doi.org/10.1093/biolre/ioab139

Qiao W et al (2019) Toxicity of perfluorooctane sulfonate on Phanerochaete chrysosporium: growth, pollutant degradation and transcriptomics. Ecotoxicol Environ Saf 174:66–74. https://doi.org/10.1016/j.ecoenv.2019.02.066

Rivera-Núñez Z et al (2023) Prenatal perfluoroalkyl substances exposure and maternal sex steroid hormones across pregnancy. Environ Res 220:115233. https://doi.org/10.1016/j.envres.2023.115233

Schönfelder G, Wittfoht W, Hopp H, Talsness CE, Paul M, Chahoud I (2002) Parent bisphenol A accumulation in the human maternal-fetal-placental unit. Environ Health Perspect. https://doi.org/10.1289/ehp.110-1241091

Shafei A et al (2018) The molecular mechanisms of action of the endocrine disrupting chemical bisphenol A in the development of cancer. Gene 647:235–243. https://doi.org/10.1016/j.gene.2018.01.016

Sobecki M et al (2016) The cell proliferation antigen Ki-67 organises heterochromatin. eLife 5:e13722. https://doi.org/10.7554/eLife.13722

Sun X, Kaufman PD (2018) Ki-67: more than a proliferation marker. Chromosoma 127:175–86. https://doi.org/10.1007/s00412-018-0659-8

Tachachartvanich P, Singam ERA, Durkin KA, Furlow JD, Smith MT, Merrill MA (2022) In Vitro characterization of the endocrine disrupting effects of per- and poly-fluoroalkyl substances (PFASs) on the human androgen receptor. J. Hazard. Mater. 429:128243. https://doi.org/10.1016/j.jhazmat.2022.128243

Tiwari SK, Agarwal S, Seth B, Yadav A, Ray RS, Mishra VN, Chaturvedi RK (2015) Inhibitory effects of bisphenol-A on neural stem cells proliferation and differentiation in the rat brain are dependent on Wnt/β-catenin pathway. Mol Neurobiol 52:1735–57. https://doi.org/10.1007/s12035-014-8940-1

Wan HT, Wong AY-M, Feng S, Wong CK-C (2020) Effects of *In Utero* Exposure to Perfluorooctane Sulfonate on Placental Functions. Environ Sci Technol 54(24):16050–16061. https://doi.org/10.1021/acs.est.0c06569

Zhang B et al (2021) Human placental cytotrophoblast epigenome dynamics over gestation and alterations in placental disease. Dev Cell 56(9):1238-1252.e5. https://doi.org/10.1016/j.devcel.2021.04.001

Zhao F, Jiang G, Wei P, Wang H, Ru S (2018) Bisphenol S exposure impairs glucose homeostasis in male zebrafish (Danio rerio). Ecotoxicol Environ Saf 147:794–802. https://doi.org/10.1016/j.ecoenv.2017.09.048

Zhou Y-T et al (2022) Perfluorooctanoic acid (PFOA) exposure affects early embryonic development and offspring oocyte quality via inducing mitochondrial dysfunction. Environ Int 167:107413. https://doi.org/10.1016/j.envint.2022.107413

Publisher's Note Springer Nature remains neutral with regard to jurisdictional claims in published maps and institutional affiliations.